



Published in final edited form as:

Biomech Model Mechanobiol. 2015 April ; 14(2): 195–215. doi:10.1007/s10237-014-0607-3.

Review. Use it or lose it: Multiscale skeletal muscle adaptation to mechanical stimuli

Katrina M. Wisdom¹, Scott L. Delp^{1,2}, and Ellen Kuhl^{1,2}

¹Department of Mechanical Engineering, Stanford University, Stanford, CA 94305, USA

²Department of Bioengineering, Stanford University, Stanford, CA 94305, USA

Abstract

Skeletal muscle undergoes continuous turnover to adapt to changes in its mechanical environment. Overload increases muscle mass, whereas underload decreases muscle mass. These changes are correlated with, and enabled by, structural alterations across the molecular, subcellular, cellular, tissue, and organ scales. Despite extensive research on muscle adaptation at the individual scales, the interaction of the underlying mechanisms across the scales remains poorly understood. Here we present a thorough review and a broad classification of multiscale muscle adaptation in response to a variety of mechanical stimuli. From this classification, we suggest that a mathematical model for skeletal muscle adaptation should include the four major stimuli, overstretch, understretch, overload, and underload, and the five key players in skeletal muscle adaptation, myosin heavy chain isoform, serial sarcomere number, parallel sarcomere number, pennation angle, and extracellular matrix composition. Including this information in multiscale computational models of muscle will shape our understanding of the interacting mechanisms of skeletal muscle adaptation across the scales. Ultimately, this will allow us to rationalize the design of exercise and rehabilitation programs, and improve the long-term success of interventional treatment in musculoskeletal disease.

Keywords

skeletal muscle; growth and remodeling; adaptation; lengthening; thickening

1 Motivation

Skeletal muscle undergoes remarkable adaptations to mechanical stimuli. Weight lifters who regularly generate large muscle forces can nearly double the size of their muscles during their careers [1]. Eccentric exercises enable muscle fiber lengthening [2, 3]. Conversely, individuals who decrease weight bearing on a lower limb experience a decrease in muscle volume [4, 5]. Chronic high heel wearers, who keep their calf muscles immobilized at short lengths, develop shorter muscles [6].

Figure 1 illustrates the multiscale architecture of skeletal muscle. Structural changes across the molecular, subcellular, cellular, tissue, and organ scales collectively contribute to macroscopic adaptations in overall muscle structure: On the molecular scale, myosin, the key contractile protein, may switch isoform types, changing the intrinsic speed of force generation [7–10]. On the subcellular scale, in response to elevated forces, more sarcomeres,

the force-producing units of muscle, are built and added in parallel, increasing muscle cross sectional area [11, 12]. Conversely, in response to disuse, sarcomeres are lost, decreasing muscle cross sectional area [5,17,18]. In response to chronic overstretch [13,14] and eccentric exercise [3,15,16], sarcomeres are added in series to cause muscle lengthening. Conversely, under-stretch initiates a decrease in sarcomeres in series and muscle shortening [6, 19–21]. On the cellular scale, the changing number of contractile units affects active force generation of muscle fibers. On the tissue scale, passive structures may respond to mechanical stimuli through changes in volume and composition, altering the overall tissue stiffnesses [22–25]. On the organ scale, the organization of muscle fibers, or muscle architecture, may change and contribute to muscle adaptation [4,5,12,26].

The complex process by which muscles adapt to mechanical stimuli spans several length scales [27]. The past three decades have generated a substantial body of literature that addresses either different length scales or different mechanical stimuli. Some overviews focus on individual length scales, either molecular [28–30], sub-cellular [31], or cellular [32–34]. Others focus on a single mechanical stimulus, for example, underload through limb suspension [35], underload in low-gravity environments [36, 37], or overload through resistance training [38–40].

Despite extensive efforts, there are almost no overviews that span multiple length scales and multiple mechanical stimuli. This is the objective of our review. By focusing on how changes across the scales cumulatively result in altered form and function, we aim to bring a unifying perspective to the process of skeletal muscle adaptation. We thoroughly review and classify muscle adaptation processes across the scales and highlight individual and mixed mechanical stimuli. Synthesizing published experimental data, we propose suitable muscle adaptation models and discuss their potential use. In the following we use the word model to refer to a mathematical model, the algebraic equation to characterize a specific phenomenon.

We acknowledge that hormonal, neural, nutritional, and metabolic factors, as well as age, gender, and species, among other factors, can significantly influence the adaptation of skeletal muscle. For the sake of clarity, we exclude these factors in this review. The tendon also plays a critical role in skeletal muscle adaptation. To focus on muscle tissue alone, we omit the tendon in the following discussion.

In the remainder of this manuscript, we adapt the following terminology: Activated muscle generates force. We specify muscle force as *isometric* if generated by a muscle maintained at constant length; as *concentric* if generated through muscle shortening; and as *eccentric* if generated through muscle lengthening. When the sarcomeres operate at their optimal length, they generate maximum force. Peak isometric muscle stress refers to the maximum isometric muscle force divided the physiological cross sectional area of the whole muscle. Peak isometric fiber stress refers to the maximum isometric fiber force divided by the fiber cross sectional area.

In what follows, we explore four types of chronic mechanical stimuli that trigger muscle adaptation: *overstretch*, the passive extension of muscle beyond its resting length; *understretch*, the passive shortening of muscle below its resting length; *overload*, the active

force generation beyond what is needed to maintain the muscle; and *underload*, the active force generation below what is needed to maintain the muscle.

2 Muscle Anatomy and Physiology

2.1 Anatomy and Physiology on the Molecular and Subcellular Scales

Sarcomeres, approximately $3 \mu\text{m}$ long assemblies of proteins, are the contractile units of skeletal muscle [41,42]. Contraction requires activity between two major protein filaments in the sarcomere: thick filaments of myosin and thin filaments of actin [44]. According to the sliding filament theory, the interdigitation of these two filaments is the mechanism of force generation [45].

Figure 2 illustrates a sarcomere unit as the region between two adjacent Z-discs [46]. The thick myosin filament is a chain joining molecules of one isoform of the myosin heavy chain protein. The primary myosin heavy chain isoforms in skeletal muscle are the slow Type I and the fast Type IIa and IIb isoforms. However, because these isoforms can switch, muscles also express intermediate, transitional isoforms [9, 47]. For different myosin heavy chain isoforms, we can model the force-velocity relationship as

$$F_{\text{fib}}^{\text{act}}(\lambda) = \frac{\beta}{(0.25 + 0.75\alpha)\lambda^{\max}} \lambda + \alpha \bar{F}, \quad (\text{Fig. 3})$$

where α is the level of muscle activation, λ^{\max} is the maximum contraction velocity, and \bar{F} is a force-length scaling factor. To account for the asymmetry between sarcomere shortening and lengthening, the parameter β varies between $\beta = \alpha F + 4F$ for shortening with $F < \alpha F$ and $\beta = 10 [\alpha F \bar{F}^{\max} - F] / [F^{\max} - 1]$ for lengthening with $F > \alpha F$ [50].

Figure 3 illustrates how the myosin heavy chain isoform affects the force-velocity relationship of skeletal muscle [47]. The curves reflect the classic response of the Hill muscle model [48–50], calibrated with human fiber experiments [62]. The different isoforms interdigitate with actin at different speeds, hence their associations as slow and fast [67]. Fiber type distribution is correlated with sensitivity of adaptation to particular stimuli, with slow muscles being sensitive to underload [69] and fast muscles being sensitive to overload [70, 71].

Myosin filaments are connected to Z-discs by a large structural protein called titin [51]. When muscle is stretched, the titin protein resists passive tension [52,53]. Titin is the main contributor to the passive force along the fiber direction on the subcellular scale [54, 55]. We can model the characteristic stretch-stiffening behavior along the fiber direction using a two-component worm-like chain model for the titin protein,

$$F_{\text{fib}}^{\text{pas}}(\lambda) = \frac{k_B T}{A} \left(\frac{1}{4(2-\lambda)^2} - \frac{5}{4} + \lambda \right), \quad (\text{Fig. 4})$$

where k_B is the Boltzmann constant, T is the absolute temperature, and A is the persistence length [51,56]. To account for the two major subregions of the titin protein, we can model titin as two wormlike chains in series with individual parameters for each subregion.

Figure 4 illustrates the passive force-stretch response for different titin isoforms. Titin isoforms may vary in length in different muscle types, but also along a single muscle [58]. The length of a particular titin subregion is related to the myosin heavy chain isoform: Longer subregions are weakly correlated with slow Type I myosin heavy chain isoforms and shorter subregions with fast Type II myosin heavy chain isoforms [58].

In addition to titin, the intermediate filament desmin, the actin and myosin filaments themselves, and the actin-myosin cross links may contribute to the passive fiber force on the subcellular scale [54, 59–61].

2.2 Anatomy and Physiology on the Cellular Scale

A muscle cell, or muscle fiber, is of cylindrical shape, between $10\ \mu\text{m}$ to $100\ \mu\text{m}$ in diameter and up to several centimeters in length [44].

Figure 5 illustrates how thousands of myofibrils, or strands of sarcomeres in series, make up a muscle fiber and account for about 80% of the total muscle fiber volume [63]. The number of sarcomeres in series and in parallel influences the muscle fiber length and cross sectional area, which, in turn, affect the cell's force-generating ability. To model the active force-length relationship, we could adapt a phenomenological multi-linear [64] or multi-quadratic [65] approach. Instead, here we motivate the active force-length relationship microscopically from actin-myosin bridging using the probability density function of a log-normal distribution,

$$F_{\text{fib}}^{\text{act}}(\lambda) = \frac{1}{\lambda\sigma\sqrt{2\pi}} \exp\left(-\frac{(\ln(\lambda) - \lambda_{\text{opt}})^2}{2\sigma^2}\right), \quad (\text{Figs. 6,7})$$

where the optimal fiber stretch λ_{opt} defines the location of the peak of the curve and the standard deviation σ defines its width.

Figure 6 illustrates the effects of adding and removing sarcomeres in series at constant fiber length, which shift the force-length curve horizontally through scaling the optimal fiber length λ_0 . Increasing or decreasing the serial sarcomere number increases or decreases the optimal fiber length at which the maximum force is generated.

Figure 7 illustrates the effects of adding and removing sarcomeres in parallel, which shift the force-length curve vertically through scaling the force F . Increasing or decreasing the parallel sarcomere number increases or decreases the fiber cross sectional area, which increases or decreases the active fiber force.

2.3 Anatomy and Physiology on the Tissue Scale

Skeletal muscle fibers are embedded in the extracellular matrix and arranged in bundles called fascicles [72]. The intramuscular connective tissue, which consists primarily of

collagen, can account for 1–10% of the total muscle mass, but may vary widely among different muscle types [22].

Figure 8 illustrates the key contributors to muscle mechanics on the tissue scale, the extracellular matrix, the endomysium surrounding each muscle fiber, the perimysium surrounding each fascicle, and the epimysium surrounding the whole muscle [73]. The extracellular matrix contributes significantly to the passive mechanical properties of skeletal muscle [74]. We can model the passive matrix force using a one-dimensional version of the classic Holzapfel model for soft biological tissue [75, 76], projected onto the collagen fiber direction,

$$F_{\text{mat}}^{\text{pas}}(\lambda) = c_0 [\lambda - 1] + \frac{c_1}{2 c_2} \exp(c_2 [\lambda - 1]^2). \quad (\text{Fig. 9})$$

In the general three-dimensional setting, the parameters c_0 and c_1 scale the isotropic and anisotropic behavior and the parameter c_2 characterizes the passive tissue nonlinearity.

Figure 9 illustrates the characteristic passive force-stretch relationship of skeletal muscle. The passive tissue force increases exponentially with increasing stretch, reflecting collagen fiber untangling [79] and collagen stiffening [80]. Increasing or decreasing the collagen content increases or decreases the passive force. As a result, changes in collagen content and collagen microstructure influence the passive resistance of the whole muscle [72, 78].

2.4 Anatomy and Physiology on the Organ Scale

Whole muscles can be several centimeter up to a few decimeters long. As illustrated in Figure 10, the cross sectional area and length of individual muscle fibers, which are closely correlated to the parallel and serial sarcomere numbers, affect the force generating ability of skeletal muscle. Muscle architecture, the three dimensional arrangement of fibers, affects the mechanical behavior on the organ scale.

A critical organ level measure of muscle architecture is the pennation angle, the angle between muscle fibers and muscle force. The pennation angle varies significantly between different muscles [82]: In muscles with a parallel muscle architecture, muscle fibers are aligned with the force-generating axis, the pennation angle is zero, and the characteristic muscle area is the anatomical cross section area. For muscles with pennate muscle architecture, muscle fibers are at an angle to the force-generation axis, and the characteristic muscle area is the physiological cross sectional area.

The active force $F_{\text{fib}}^{\text{act}}$ from Figures 6 and 7, scaled by the active force-velocity relationship in Figure 3, supplemented by the passive force-length relationships on the cellular and tissue scales $F_{\text{fib}}^{\text{pas}}$ and $F_{\text{mat}}^{\text{pas}}$ in Figures 4 and 9, collectively characterize skeletal muscle mechanics on the organ scale. Fig. 11 illustrates the total muscle force,

$$F(\lambda) = F_{\text{fib}}^{\text{act}} + F_{\text{fib}}^{\text{pas}} + F_{\text{mat}}^{\text{pas}}, \quad (\text{Fig. 11})$$

which captures the peak and drop of the active cell force $F_{\text{fib}}^{\text{act}}$ and the drastic stiffening of the passive cellular and extracellular matrix forces $F_{\text{fib}}^{\text{pas}}$ and $F_{\text{mat}}^{\text{pas}}$.

3 Muscle Physiology of Adaptation

Table 1 summarizes the literature on multiscale muscle adaptation to various mechanical stimuli in animals and humans. In the following subsections, we discuss these mechanisms in detail.

3.1 Physiology of Adaptation on the Molecular and Subcellular Scales

Adaptation of Myosin Heavy Chain Isoform—The myosin heavy chain isoform expression in skeletal muscle can change in response to mechanical cues. Muscle remodeling in favor of a greater percentage of slower myosin heavy chain isoforms occurs in animals subjected to stretch, overload, and eccentric exercise [8,10,47,147]. Animal experiments have also shown that the sarcomeres added in response to overload express primarily the slow myosin heavy chain isoform [103].

In humans, myosin heavy chain adaptation is not as well understood. Some studies reported shifts toward slower isoforms in response to sufficient overload [7, 9, 102, 113] while others found no significant change [26, 110]. In response to underload, limb unweighting [113], bed rest [134,135], and microgravity [145,146] display mixed results. Some studies reported a fractional decrease in slow-twitch fibers and a fractional increase in fast-twitch fibers [113,140,145,146], while other studies found no change [134, 135].

Level of neural activation is a major difference among these disuse models. This presents a problem because muscle adaptation can be regulated by neural signals [66,148] and even neural factors unrelated to the activation level [149, 150]. Most studies do not involve completely severing the nervous system connection. This implies that neural activation remains possible, even in complete unloading [151]. Several studies have isolated the effect of neural factors with constant levels of disuse, and have found more dramatic shifts toward faster myosin heavy chain isoforms in the absence of these signals [149, 152]. Approximately 40% of type I MHC composition of the adult rat soleus has been attributed to activation-related events, implicating variation in neural factors among disuse experiments as a major contributor to discrepancies in results [149].

Adaptation of Titin Protein Isoform—Despite intense studies, our understanding of how the titin protein may adapt to mechanical stimuli is still incomplete [153]. Underload experiments in rat have reported mixed results; one study has shown that titin isoform size and density decrease [129], while other studies found decreased density but not length [130] or no change in length or density, but an apparent decrease in elasticity [131]. Although titin isoform size is weakly correlated to myosin heavy chain type [57], the precise effect of titin adaptation on overall muscle function is still under intense debate [153]. It is clear though that titin adaptation has similar effects as extracellular matrix adaptation: It primarily affects the passive force contribution.

Adaptation of Serial Sarcomere Number—Overstretch and understretch of skeletal muscle initiate an increase and decrease, respectively, in the serial sarcomere number [6, 13, 19, 20, 88, 101]. Figure 6 illustrates the effect of serial sarcomere number adaptation.

Serial sarcomere numbers increase in response to immobilization in a stretched position [20, 88] and limb lengthening [13, 14, 85, 86]. It is well accepted that passive stretch beyond a physiological threshold initiates the process of sarcomerogenesis through a series of cellular and molecular events [154]. However, the precise sequence of mechanotransduction pathways that triggers serial sarcomere adaptation remains largely unknown [155]. It has been hypothesized that the sarcomere number changes to re-establish the optimal sarcomere length, the length at which maximal force production occurs [156]. Sarcomeres are primarily added at myotendinous junctions, although it may be possible for them to be added throughout the length of a muscle fiber [88, 154].

Increased sarcomere lengths, rather than sarcomere numbers, have been observed in a few studies, indicating that adaptation to the overstretch may have been incomplete or partially unsuccessful [84,85]. Failure of a muscle to properly adapt to the overstretch it experiences may result in contracture, or insufficient muscle length [85]. Contracture is one of the most common, and painful, complications of limb lengthening surgery [83, 85].

Because muscle protein synthesis increases more dramatically in stretched and stimulated muscle than in stretched and unstimulated muscle [96,157], active overstretch triggers serial sarcomere addition to a greater extent than passive overstretch [16]. In rats, eccentric exercise triggers serial sarcomere deposition [3]. In humans, eccentric resistance training also leads to serial sarcomere deposition and enables significant fascicle lengthening [15, 16]. This increase in muscle length enables increased range of motion. Sarcomerogenesis serves as a major subcellular mechanism to reposition the muscle to its optimal position within the new force-length relationship [88, 98, 158].

In response to chronic understretch, the serial sarcomere number decreases. Various animal studies have demonstrated this effect [19–21, 88, 97, 98]. Humans who experience partial or total muscle immobilization [101], for example by frequently wearing high heels [6], may experience chronic muscle shortening caused by a decrease of sarcomeres in series.

Adaptation of Parallel Sarcomere Number—We commonly assume that cross sectional area is directly correlated to the number of sarcomeres in parallel [17, 81, 155, 159]. With the exceptions of steroid-induced hypertrophy [160] or blockage of the transforming growth factor- β family member myostatin [161], this implies that an increase in cross sectional area of skeletal muscle fibers indicates the addition of sarcomeres in parallel. An array of studies measure increases or decreases in fiber cross sectional area, and these results are taken as evidence of parallel sarcomere addition or resorption. In particular, functional overload through targeted muscle removal in animals, e.g. synergist removal [11] or surgical ablation, and through resistance exercise [12, 26, 112] trigger parallel sarcomere deposition. By contrast, disuse initiates parallel sarcomere removal [17].

3.2 Physiology of Adaptation on the Cellular Scale

Adaptation of Cross Sectional Area—Increase in fiber cross sectional area, or fiber hypertrophy, is correlated to the number of sarcomeres added in parallel. Figure 7 illustrates the effect of fiber cross sectional area adaptation. Chronic overloading in animals initiates an increase in fiber cross sectional area [11]. This effect has been recently confirmed in humans in response to resistance exercise [12,26,112]. The observation that protein synthesis increases in response to resistance exercise supports the hypothesis that the increase in cross section reflects an increase in contractile material, and thus in force-generating ability, as illustrated in Figure 7 [104, 105]. The increase in satellite cells following resistance exercise may provide the machinery for increased manufacturing of this contractile material [106]. Recent studies have emphasized the role of miRNAs in mediating the response and adaptation of skeletal muscle to various modes of exercise [107]. Underload initiates a decrease in fiber cross sectional area, but results vary by disuse model. Some studies of bed rest [134–136], space-flight [142, 143], immobilization in humans [18, 141] and hindlimb suspension in animals [125] have seen decrease in cross sectional area across all fiber types. Other animal hindlimb suspension models have shown pronounced atrophy only in slow twitch fibers [123,126]. Animal age appears to influence the adaptive response of the fiber cross sectional area [125]; fibers in aged animals may experience delayed atrophy [162].

The unclear extent to which neural activation is inhibited may prevent direct comparison among unloading studies [128]. Rat experiments on inactivity with and without spinal cord separation have shown that activation-related events account for at least 75% of the decrease in fiber size [149].

Homeostatic cross sectional area results from balanced protein synthesis and protein breakdown. Studies indicate that the primary contributor to disuse atrophy is a decrease in protein synthesis rather than an increase in protein breakdown. This imbalance causes a net loss of protein mass and cross sectional area of individual muscle fibers [141]. Both decreased signaling for protein synthesis (decreased demand) or decreased number of satellite cells following atrophy (decreased supply of protein synthesis machinery) may contribute to the atrophy [163].

Adaptation of Peak Isometric Fiber Stress—Peak isometric fiber stress may change in response to mechanical stimuli. Muscle adaptation to long duration resistance training can initiate an increase in peak isometric fiber stress [110]. By contrast, underload induced by limb unweighting [128], immobilization [140], bed rest [136, 137], and microgravity [143] initiates a decrease. In one study, the decrease in peak isometric fiber stress linearly correlated with the decrease in myosin concentration following underload [140]. Declines in the number of actin-myosin cross-bridges per fiber [140,143] and in strength per cross-bridge following disuse [47] contribute to the loss in muscle strength in response to underload [122]. Further research is needed to identify other contributors to specific tension of the muscle fiber and quantify their importance and plasticity.

Adaptation of Fiber Type—Delineating muscle fiber types by myosin heavy chain isoform expression profile is most common, although fiber types exhibit differences in

metabolic rates, oxidative properties, and isoform expression of other sarcomeric proteins [66]. The changes in myosin heavy chain isoform on the molecular scale, alongside these other factors, allow for whole fiber type transitions in response to mechanical stimuli.

Functional overload [119] and overstretch [10,89] are potent initiators of transition to slow twitch fiber types in animal muscle. Similarly, slow-to-fast fiber type transitions occur in animals subjected to underload [127, 144]. Generally, fast fiber types respond more drastically to overload and overstretch, and slow fiber types respond more drastically underload induced changes [66, 128].

In humans, fiber type transitions, especially in response to underload, are less consistent than in animals [18, 113, 117, 120, 134, 135, 140, 145]. Mixed stimuli, variations in neural activity, and different methods of fiber type classification may obfuscate results in adaptive human fiber type transitions [66]. Some experimental stimuli may be insufficient, whereas a three month regimen of heavy-load resistance training successfully initiates transitions to slower fiber types [113, 117]. Elite, high-endurance athletes such as long distance runners have high percentages of slow fibers [164], and sprinters and power-weight lifters, who require speed over endurance, have high percentages of fast fibers [164], which seem to support the “sufficient stimulus” hypothesis. However, genetics may partially explain endowment of fiber types [30,120,165]. Despite extensive research, quantitative characterization of the conditions under which fiber type transitions definitively occur in humans is still lacking.

Fiber type adaptation affects both force generating capacity and sensitivity to future adaptation. Although some studies have noted differences in peak isometric force among fast- and slow-twitch fibers [27, 166, 167], differences in the force-velocity relationship among these fibers, illustrated in Figure 3, contribute to larger force discrepancies, particularly at high shortening and lengthening velocities. Even so, fiber type percentage has a smaller effect on whole muscle force, in comparison to other parameters, such as muscle length, cross sectional area, and pennation angle, as long as velocity of contraction does not approach maximum shortening or lengthening (Figure 3) [44, 158]. Predominantly slow-twitch muscles are more responsive to underload [69], and that fast-twitch muscles are more sensitive to overload [70,71]. Switching myosin heavy chain isoforms and fiber types may thus incrementally alter a muscle’s sensitivity to further adaptation.

3.3 Physiology of Adaptation on the Tissue Scale

Adaptation of Extracellular Matrix Volume—Extracellular matrix, through volume, structure, and stiffness variation, adapts in response to mechanical stimuli [22, 118]. Figure 9 illustrates the effect of extracellular matrix stiffening on the passive force-length properties of skeletal muscle.

Chronic overload, overstretch, and understretch all initiate an increase in the passive stiffness of skeletal muscle [20, 22–25, 95, 97, 114]. Increased passive stiffness can be facilitated through increased extracellular matrix volume [87, 100], especially that which is enabled by increased collagen content [22, 23, 118]. Because collagen is so stiff in comparison to skeletal muscle fibers, a change in collagen content can noticeably alter the

passive mechanical properties of skeletal muscle [167]. Further increase in tissue stiffness can arise through reorientation of collagen fibers [100]. In animal models, changes in extracellular matrix chemistry and fiber cross-linking also alter its passive stiffness [168–170]. Several different mechanisms operate in the regulation of extracellular matrix properties.

Stretch regimens show inconsistent results. This may be because tendon compliance changes in response to mechanical stimuli in conjunction with, or instead of, skeletal muscle passive stiffness [22,92,93]. Passive muscle stiffness is different from range of motion, which is improved through stretching and is associated with improved tendon compliance rather than decreased passive muscle stiffness [171, 172].

Many questions remain unanswered regarding the underlying mechanisms of extracellular matrix remodeling [173]. However, it is clear that this adaptation contributes significantly to changes of whole muscle properties. Increased stiffness increases load resistance and renders connective tissue more damage resistant, particularly within a remodeling muscle [22]. Increased extracellular matrix may be a temporary response to the injury induced by extreme mechanical stimuli [25, 174]. Extracellular matrix turnover in general facilitates cell migration, formation of new muscle, and reorganization of the extracellular matrix, events necessary for muscle adaptation [174]. Accumulation or depletion of connective tissue in skeletal muscle may further enable adjustment of the relative importance of the titin protein (Figure 4) and extracellular matrix material (Figure 9) to passive properties of skeletal muscle as a whole (Figure 11) [153].

3.4 Physiology of Adaptation on the Organ Scale

The consequences of adaptation to mechanical stimuli on the smaller scales collectively contribute to changes on the whole muscle scale.

Adaptation of Anatomical Cross Sectional Area and Volume—Overload induced by resistance exercise leads to increased anatomical cross sectional area [11,12,15,16,26, 105,108,109,111,115] and whole muscle volume [26,108] in both humans and animals. Subjects in eccentric and concentric training studies experience a greater increase in muscle mass in response to high intensity eccentric training than in response to concentric training [38]. This motivated the hypothesis that the higher absolute loads generated during eccentric contractions are the critically important mechanical stimuli [38, 175]. Controlled animal studies have revealed that intermittent passive stretch may trigger both radial and longitudinal growth [96]. However, this observation may be the result of passive stretch in the presence of rapid natural growth experienced by small rodents [120]. In humans, passive stretch does not induce significant protein synthesis or hypertrophy [176]. What initiates hypertrophy is not well understood; competing hypotheses suggest that either active strain [176] or fiber stress [68] may regulate anatomical cross sectional area.

Underload initiated by disuse causes a drastic decrease in anatomical cross sectional area [4, 5, 18, 121, 122, 132, 133] and whole muscle volume [4, 5, 121]. Two months of disuse can cause a muscle to atrophy to half of its normal size [177]. Limited literature is available on the effect of understretch with continued muscle loading, although this situation is

commonly experienced in humans by chronic high-heel wearers [6]. Although muscles in chronic high-heel wearers shorten, the cross sectional area of these muscles does not significantly change [6].

Increase and decrease in fiber cross sectional area translate directly into increase and decrease of anatomical cross sectional area via the pennation angle.

Adaptation of Pennation Angle—Pennation angle can vary among different muscles and is highly plastic [155]. Muscle adaptation can include a reorientation of muscle fibers in addition to changes in fiber geometry. Fiber reorientation may affect both the amount of force that can be exerted over a cross sectional area and the transmission of force among the individual fibers [16, 178].

Increased pennation angle is positively correlated with increased sarcomeres in parallel, negatively correlated with the number of sarcomeres in series, and can change with muscle hypertrophy [12, 15, 16, 26, 108]. These observations motivate the hypothesis that the fascicle angle adapts to accommodate hypertrophy within the limited space available in the whole muscle [15, 26, 178]. For a muscle of constant fascicle length, fiber length, and fiber number, experimental evidence indicates that an increase in fiber diameter is correlated to an increase in pennation angle [179, 180]. This fiber-packing strategy allows for maximizing the number of contractile elements attached to a tendon [158, 179]. As expected, an underload induced decrease in anatomical cross sectional area results in a decrease in pennation angle [4, 5, 121, 122].

Adaptation of Fascicle Length—Eccentric exercise initiates fascicle lengthening [2,15,16], whereas understretch, e.g. in chronic high heel wearing, initiates fascicle shortening [6]. The extent to which the lengthening or shortening of myofibrils, i.e. the addition or resorption of sarcomeres in series, contributes to the change in fascicle length depends on the pennation angle.

The relationships between fascicle length and pennation angle and between pennation angle and anatomical cross sectional area indicate that whole muscle adaptation is simultaneously dependent on both muscle length and cross sectional area. For example, in the presence of underload and understretch, e.g. during immobilization in a shortened position, rat muscle cross sectional area decreases [19]. A controlled animal model has shown that in the highly pennated gastrocnemius, cross sectional area changes alone proved sufficient to establish a new muscle force-length relationship without the removal of sarcomeres in series [19]. In the unipennate soleus, however, cross sectional area changes alone were insufficient to induce the required change in length, and a removal of sarcomeres in series was necessary. These studies affirm the crucial role of architectural remodeling in skeletal muscle adaptation.

Adaptation of Peak Isometric Muscle Stress—Overload increases peak isometric muscle stress [108], whereas limb unweighting [121] and immobilization [18] decrease peak isometric muscle stress. Adaptation to peak isometric fiber stress likely scales up to the organ scale [110, 137, 140].

4 Modeling Muscle Adaptation

The past two decades have seen significant advancements in skeletal muscle modeling. Global, three-dimensional models of electrical activation and mechanical contraction now provide great insight into muscle anatomy, structure, and function on multiple scales [181–187]. Local models complement this insight by studying the interaction among the biochemistry, metabolism, and force production in skeletal muscle [188, 189]. However, muscle models that reliably predict the long-term response of skeletal muscle are still surprisingly rare [190, 191]. A recent study focused on modeling the adaptation of skeletal muscle in response to chronic understretch and overstretch [192]. This pioneering work provided valuable insight, but was limited to a one-dimensional model.

First attempts to simulate the chronic adaptation of skeletal muscle in a fully three-dimensional setting using a multiscale, multifield model are currently underway [193]. These models rely on a three-step procedure: First, they project global, whole muscle strain and stress onto local subcellular stretch and force using microstructural information such as volume fractions and pennation angles. Second, they locally evaluate the biochemistry and metabolism on the cellular scale, for example, by simulating the deposition or removal of sarcomeres in series or in parallel to predict the resulting stretch and force. Third, they recollect this information and translate local cellular stretch and force back to global, whole muscle strain and stress using microstructural information [194]. Key to this method is the modularity of the second step, which enables the seamless integration of various cellular and molecular processes into a whole muscle model [195]. Finite element methods are typically the first choice to naturally embed this approach by modeling the whole muscle and tissue information globally at the node point level and integrating the cellular and molecular processes locally at the integration point level [196, 197]. In the following subsections, we suggest possible muscle adaptation models in response to chronic overstretch, overload, and underload, and compare them against experimental and clinical data.

4.1 Modeling Adaptation to Overstretch

To model skeletal muscle adaptation in response to chronic overstretch, we consult experiments of chronic limb lengthening [198]. In these experiments, the serial sarcomere number increased exponentially, and then converged toward a homeostatic equilibrium value, which was correlated to the amount of overstretch. This motivates the following equation for changes in serial sarcomere number in response to overstretch [193],

$$\dot{n}(t) = \frac{1}{\tau} \left(\frac{n^{\max} - n}{n^{\max} - 1} \right)^{\gamma} (\lambda^e - \lambda^o). \quad (\text{Fig. 12})$$

Here n is the serial sarcomere number, n^{\max} is its limiting value, τ is a time constant that controls the adaptation speed, and γ controls the nonlinearity of the adaptation process. The switch factor $(\lambda^e - \lambda^o)$ controls the amount of overstretch and activates the serial addition of sarcomeres only if the elastic muscle stretch λ^e exceeds the physiological baseline value λ^o .

Figure 12 illustrates the gradual increase in serial sarcomere number in response to long-term overstretch. On the subcellular scale, the sarcomere number increases gradually to

reduce the sarcomere stretch λ^e and to reposition the sarcomere and the muscle fiber back into their optimal operating regime [199]. On the organ scale, the muscle increases in length to compensate for the amount of overstretch or passive force [190]. Increasing or decreasing the amount of overstretch increases or decreases the serial sarcomere number. The model, shown as black dashed line, captures the general trend observed during chronic limb lengthening experiments in rabbits, shown as red circles, where the serial sarcomere number increased by 14% to compensate for the chronically applied overstretch of $\lambda = 1.14$ [198].

4.2 Modeling Adaptation to Overload

To model skeletal muscle adaptation in response to chronic overload, we examine results of training protocols, in which the muscle cross sectional area of the human thigh was measured throughout a period of eight weeks of training [201]. In these experiments, the cross sectional area increased exponentially, and then converged toward a homeostatic equilibrium value. In analogy to the previous section, we can introduce the following equation for changes in cross sectional area in response to chronic overload [200],

$$\dot{A}(t) = \frac{1}{\tau} \left(\frac{A^{\max} - A}{A^{\max} - 1} \right)^{\gamma} (F - F^o). \quad (\text{Fig. 13})$$

Here A is the cross sectional area, A^{\max} is its limiting value, τ is a time constant that controls the adaptation speed, and γ controls the nonlinearity of the adaptation process. Conceptually similar to overstretch, we have introduced a switch factor $(F - F^o)$ to control the amount of overload. It activates the parallel addition of sarcomeres only if the total muscle force F exceeds the physiological baseline value F^o .

Figure 13 illustrates the gradual increase in cross sectional area in response to long-term training. On the organ scale, the muscle increases its cross sectional area to compensate for the amount of overload or active force [190]. On the subcellular scale these changes are brought about by the parallel addition of sarcomeres, which form additional myofibrils to increase the overall cross sectional area. Increasing or decreasing the overload increases or decreases the cross sectional area. The model, shown as black dashed line, agrees well with exercise protocols in humans, shown as red circles, where the cross sectional area of the right thigh muscles increased by 9.59%, from 145 cm² to 158.9 cm², in response to overload generated by exercise [201].

4.3 Modeling Adaptation to Understretch or Underload

To model skeletal muscle adaptation in response to chronic understretch or underload, we consult measurements of patients of the intensive care unit who underwent bed rest over periods of up to 100 days [202]. In these patients, the muscle layer thickness decreased exponentially, and then converged toward a minimum baseline value. This motivates the following exponential equation for muscle loss in response to chronic under-stretch or underload,

$$\dot{V}(t) = -\frac{1}{\tau}(1 - V^{\min})\exp(-t/\tau). \quad (\text{Fig. 14})$$

Here V is the normalized muscle volume and V^{\min} is its minimum baseline value. The time parameter τ , which controls the adaptation speed, can either have a constant value or be a function of the amount of understretch $\tau(\lambda)$ or underload $\tau(F)$. The exponential nature of the muscle loss equation enables its explicit integration to obtain the following direct expression for the whole muscle volume as a function of time, $V(t) = (1 - V^{\min}) \exp(-t/\tau)$. Figure 14 illustrates the gradual loss of muscle volume in response to long-term bed rest. On the organ scale, muscle decreases its volume and mass to compensate for the amount of underload. On the subcellular scale, understretch and underload initiate the serial and parallel removal of sarcomeres. Increasing or decreasing the amount of understretch λ or underload F increases or decreases the speed of muscle volume loss τ as shown in blue and green. This model, shown as black dashed line, captures the trend of the skeletal muscle loss in bedridden hospital patients, shown as red circles [202]. Using an exponentially decaying function to model muscle loss as a function of disuse time is supported by prior work, in which an exponential function was utilized to model fiber volume, obtained by biopsy, as a function of time of immobilization [141]. In this prior study, fiber volume loss was proportional to loss in protein mass [141]. This illustrates that muscle atrophy propagates across the scales, from protein mass via fiber volume to whole muscle volume. These phenomena support the use of exponential multiscale models to characterize muscle loss in response to understretch or underload.

5 Discussion

In this review, we have discussed current challenges in modeling skeletal muscle adaptation. The major roadblock toward reliable, predictive modeling of muscle adaptation is the lack of adequate experimental data with sufficient resolution in both space and time. Most existing data sets on skeletal muscle adaptation report information of a single spatial scale. To truly link cause and effect, it would be critical to characterize the adaptation process across multiple spatial scales. In addition, almost all existing studies are limited to only two time points, the initiation of the adaptation process at time zero and the result at a later time point. To create mathematical models that reliably predict the progression of the muscle adaptation, it would be important to characterize the adaptation process at multiple points in time.

After our thorough literature review, we suggest the following set of experiments to provide insight into the time line of chronic muscle adaptation: i) monitoring the serial sarcomere number, fiber length, and whole muscle length upon progressive overstretch at multiple time points [198] similar to Figure 12, but now by gradually increasing the magnitude of stretch; ii) monitoring the parallel sarcomere number, fiber cross sectional area, and anatomical cross sectional area at multiple time points [201] similar to Figure 13, but now by gradually increasing the magnitude of load; and iii) monitoring the total sarcomere number, fiber size, and muscle volume upon understretch and underload at multiple time points [202] similar to Figure 14. On the subcellular scale, recent developments in microendoscopy now enable non-invasive sarcomere imaging both in animals and humans, to characterize changes in

serial and parallel sarcomere number in vivo [41,42]. On the cellular, tissue, and organ scales, features such as fascicle length, pennation angle, and muscle thickness can be characterized non-invasively in vivo using ultrasound [43].

The measured data sets could then be collectively integrated into a unified, holistic multiscale model of chronic muscle adaptation, which should at least include the following information: i) at the molecular and sub-cellular scales: changes in myosin heavy chain isoform, which affect active muscle velocity according to Figure 3; ii) at the cellular scale: changes in serial sarcomere number, which affect fascicle length and active muscle force according to Figure 6; iii) at the cellular scale: changes in parallel sarcomere number, which affect anatomical cross sectional area and active muscle force according to Figure 7; iv) at the tissue scale: changes in extracellular matrix volume, structure, and composition, which affect passive muscle stiffness according to Figure 9; v) at the organ scale: changes in pennation angle, which affect anatomical cross sectional area and active muscle force. Taken together, these changes in myosin heavy chain isoform, fiber length, fiber cross sectional area, extracellular matrix stiffness, and pennation angle collectively impair the adaptation of overall muscle form and function.

A model like this includes five key players in chronic muscle adaptation to mechanical stimuli, but it is, of course, not comprehensive. The following information could be included in a more advanced model of chronic muscle adaptation: vi) at the molecular scale: changes in titin isoform [129–131]; vii) at the subcellular scale: changes in number [140,143] and force [47] of actomyosin cross-bridges within the sarcomeres; viii) at the cellular scale: changes in desmin protein content, as desmin also affects passive myofibril stiffness [59–61]; ix) at the organ scale: changes in collagen fiber orientation and extracellular matrix composition [203, 204]; ix) at the organ scale: changes in tendon geometry and tendon stiffness, which affect passive mechanical properties of the muscle-tendon unit [205]. Beyond the organ scale, this approach does not yet address the wide variety of factors that influence muscle adaptation at larger, more integrative scales. This includes muscle-specific architecture, attachment geometry, and function [206], as well as subject-specific neural factors, age, gender, species, nutrition, and hormone levels [207]. These factors may significantly affect adaptation [18, 125, 208, 209].

The major advantage of multiscale modeling, in comparison to individual single scale modeling, is that it will provide a more holistic understanding of skeletal muscle adaptation. Ultimately, multiscale models have the potential to explain mechanisms by using parameters that have a clear physical interpretation, rather than using phenomenological parameters that are based on data fitting. For example, multiscale modeling could provide useful bounds on the speed of muscle growth or identify the energy required to build a specific amount of new muscle by using assembly kinetics from the molecular and subcellular scales.

6 Conclusion

This review has systematically categorized skeletal muscle adaptation in response to various mechanical stimuli from the molecular to the organ scale. From this classification, we have identified four major driving mechanisms of skeletal muscle adaptation: overstretch,

understretch, overload, and underload; and five key players in skeletal muscle adaptation: changes in myosin heavy chain isoform, serial sarcomere number, parallel sarcomere number, pennation angle, and extracellular matrix composition. We have highlighted major dependencies among these variables and the initiators of changes within them. We have discussed the adaptation with respect to isolated and combined mechanical stimuli, and reviewed protocols to study their impact in animal models and in human health, training, and rehabilitation. From the insight gained through these studies, we have suggested three muscle adaptation models in response to overstretch, overload, and underload. Mathematical modeling has a tremendous potential in understanding skeletal muscle adaptation across the scales. Computational modeling can naturally integrate the mechanobiology of muscle adaptation at the molecular, subcellular, and cellular scales into the biomechanics at the organ and tissue scales. Computer models not only provide detailed insight into the interacting mechanisms of muscle adaptation; they can also serve as valuable tools to predict outcomes of pharmaceutical or interventional treatment, and help design individualized training, treatment, and rehabilitation plans.

Acknowledgments

This work was supported by the National Science Foundation Graduate Research Fellowship and by the Stanford Graduate Engineering Fellowship to Katrina Wisdom, by the National Institutes of Health grants R24 HD065690 and U54 GM072970 to Scott Delp, and by the National Science Foundation CAREER award CMMI 0952021 and INSPIRE grant 1233054 and by the National Institutes of Health grant U01 HL119578 to Ellen Kuhl. Thank you to Dr. Richard Lieber, Alexander Real, Aleksandra Denisin, and Alexander Zöllner for helpful conversations, and to David Delp for the illustrations.

References

1. D'Antona G, Lanfranconi F, Pellegrino MA, Brocca L, Adami R, et al. Skeletal muscle hypertrophy and structure and function of skeletal muscle fibres in male body builders. *J Physiol*. 2006; 570:611–627. [PubMed: 16339176]
2. Brockett CL, Morgan DL, Proske U. Human hamstring muscles adapt to eccentric exercise by changing optimum length. *Med Sci Sports Exerc*. 2001; 33:783–790. [PubMed: 11323549]
3. Lynn R, Morgan D. Decline running produces more sarcomeres in rat vastus intermedius muscle fibers than does incline running. *J Appl Physiol*. 1994; 77:1439–1444. [PubMed: 7836150]
4. Psatha M, Wu Z, Gammie FM, Ratkevicius A, Wackerhage H, et al. A longitudinal MRI study of muscle atrophy during lower leg immobilization following ankle fracture. *J Magn Reson Imaging*. 2012; 35:686–695. [PubMed: 22045592]
5. Campbell EL, Seynnes OR, Bottinelli R, McPhee JS, Atherton PJ, et al. Skeletal muscle adaptations to physical inactivity and subsequent retraining in young men. *Biogerontology*. 2013; 14:247–259. [PubMed: 23666342]
6. Csapo R, Maganaris CN, Seynnes OR, Narici MV. On muscle, tendon and high heels. *J Exp Biol*. 2010; 213:2582–2588. [PubMed: 20639419]
7. Jürimäe J, Abernethy PJ, Blake K, McEniery MT. Changes in the myosin heavy chain isoform profile of the triceps brachii muscle following 12 weeks of resistance training. *Eur J Appl Physiol Occup Physiol*. 1996; 74:287–292. [PubMed: 8897036]
8. Goldspink G, Scutt A. Gene expression in skeletal muscle in response to stretch and force generation. *Am J Physiol Integr Comp Physiol*. 1992; 262:R356–R363.
9. Williamson D. Reduction in hybrid single muscle fiber proportions with resistance training in humans. *J Appl Physiol*. 2001; 91:1955–1961. [PubMed: 11641330]
10. De Deyne PG, Hayatsu K, Meyer R, Paley D, Herzenberg JE. Muscle regeneration and fiber-type transformation during distraction osteogenesis. *J Orthop Res O3 Publ Orthop Res Soc*. 1999; 17:560–570.

11. Johnson T, Klueber K. Skeletal muscle following tonic overload: functional and structural analysis. *Med Sci Sports Exerc.* 1991; 23:49–55. [PubMed: 1997813]
12. Farup J, Kjølhed T, Sørensen H, Dalgas U, Møller AB, et al. Muscle morphological and strength adaptations to endurance vs. resistance training. *J Strength Cond Res.* 2012; 26:398–407. [PubMed: 22266546]
13. Boakes JL, Foran J, Ward SR, Lieber RL. Muscle adaptation by serial sarcomere addition 1 year after femoral lengthening. *Clin Orthop Relat Res.* 2007; 456:250–253. [PubMed: 17065842]
14. Lindsey CA, Makarov MR, Shoemaker S, Birch JG, Buschang PH, et al. The effect of the amount of limb lengthening on skeletal muscle. *Clin Orthop Relat Res.* 2002; 402:278–287. [PubMed: 12218494]
15. Blazeovich AJ, Cannavan D, Coleman DR, Horne S. Influence of concentric and eccentric resistance training on architectural adaptation in human quadriceps muscles. *J Appl Physiol.* 2007; 103:1565–1575. [PubMed: 17717119]
16. Seynnes OR, de Boer M, Narici MV. Early skeletal muscle hypertrophy and architectural changes in response to high-intensity resistance training. *J Appl Physiol.* 2007; 102:368–373. [PubMed: 17053104]
17. Narici MV, Maganaris CN. Plasticity of the muscle-tendon complex with disuse and aging. *Exerc Sport Sci Rev.* 2007; 35:126–134. [PubMed: 17620931]
18. Yasuda N, Glover EI, Phillips SM, Isfort RJ, Tarnopolsky MA. Sex-based differences in skeletal muscle function and morphology with short-term limb immobilization. *J Appl Physiol.* 2005; 99:1085–1092. [PubMed: 15860685]
19. Heslinga JW, te Kronnie G, Huijijng PA. Growth and immobilization effects on sarcomeres: a comparison between gastrocnemius and soleus muscles of the adult rat. *Eur J Appl Physiol Occup Physiol.* 1995; 70:49–57. [PubMed: 7729438]
20. Tabary J, Tabary C, Tardieu C. Physiological and structural changes in the cat's soleus muscle due to immobilization at different lengths by plaster casts. *J Physiol.* 1972; 224:231–244. [PubMed: 5039983]
21. Baker JH, Matsumoto DE. Adaptation of skeletal muscle to immobilization in a shortened position. *Muscle Nerve.* 1988; 11:231–244. [PubMed: 3352658]
22. Kjaer M. Role of extracellular matrix in adaptation of tendon and skeletal muscle to mechanical loading. *Physiol Rev.* 2004; 84:649–698. [PubMed: 15044685]
23. Williams P, Kyberd P, Simpson H, Kenwright J, Goldspink G. The morphological basis of increased stiffness of rabbit tibialis anterior muscles during surgical limb lengthening. *J Anat.* 1998; 193:131–138. [PubMed: 9758143]
24. Tardieu C, Tabary JC, Tabary C, Tardieu G. Adaptation of connective tissue length to immobilization in the lengthened and shortened positions in cat soleus muscle. *J Physiol (Paris).* 1982; 78:214–220. [PubMed: 7131334]
25. Hoang PD, Herbert RD, Gandevia SC. Effects of eccentric exercise on passive mechanical properties of human gastrocnemius in vivo. *Med Sci Sports Exerc.* 2007; 39:849–857. [PubMed: 17468585]
26. Aagaard P, Andersen JL, Dyhre-Poulsen P, Leffers AM, Wagner A, et al. A mechanism for increased contractile strength of human pennate muscle in response to strength training: changes in muscle architecture. *J Physiol.* 2001; 534:613–623. [PubMed: 11454977]
27. Taber LA. Biomechanics of Growth, Remodeling, and Morphogenesis. *Appl Mech Rev.* 1995; 48:487–545.
28. Haddad F, Roy R. Atrophy responses to muscle inactivity. II. Molecular markers of protein deficits. *J Appl Physiol.* 2003; 95:791–802. [PubMed: 12716877]
29. Billeter R, Puntschort A, Vogt M, Wittwer M, Wey E. Molecular Biology of Human Muscle Adaptation. *Int J Sports Med.* 1997; 18:S300–S301. [PubMed: 9391840]
30. Baldwin K, Haddad F. Invited Review: Effects of different activity and inactivity paradigms on myosin heavy chain gene expression in striated muscle. *J Appl Physiol.* 2001; 90:345–357. [PubMed: 11133928]
31. Ehler, E.; Gautel, M. *Sarcomere Skelet Muscle Dis.* Springer; 2008. The sarcomere and sarcomerogenesis; p. 1-14.

32. Haddad F, Roy RR, Zhong H, Edgerton VR, Baldwin KM. Atrophy responses to muscle inactivity. I. Cellular markers of protein deficits. *J Appl Physiol.* 2003; 95:781–790. [PubMed: 12716870]
33. Tidball JG. Mechanical signal transduction in skeletal muscle growth and adaptation. *J Appl Physiol.* 2005; 98:1900–1908. [PubMed: 15829723]
34. Carson JA, Wei L. Integrin signaling's potential for mediating gene expression in hypertrophying skeletal muscle. *J Appl Physiol.* 2000; 88:337–343. [PubMed: 10642399]
35. Hackney KJ, Ploutz-Snyder LL. Unilateral lower limb suspension: integrative physiological knowledge from the past 20 years (1991–2011). *Eur J Appl Physiol.* 2012; 112:9–22. [PubMed: 21533809]
36. Adams GR, Caiozzo VJ, Baldwin KM. Skeletal muscle unweighting: spaceflight and ground-based models. *J Appl Physiol.* 2003; 95:2185–2201. [PubMed: 14600160]
37. Trappe S. Effects of Spaceflight, Simulated Space-flight and Countermeasures on Single Muscle Fiber Physiology. *J Gravitational Physiol.* 2002; 9:323–326.
38. Roig M, O'Brien K, Kirk G, Murray R, McKinnon P, et al. The effects of eccentric versus concentric resistance training on muscle strength and mass in healthy adults: a systematic review with meta-analysis. *Br J Sports Med.* 2009; 43:556–568. [PubMed: 18981046]
39. Hedayatpour N, Falla D. Non-uniform muscle adaptations to eccentric exercise and the implications for training and sport. *J Electromyogr Kinesiol O3 J Int Soc Electrophysiol Kinesiol.* 2012; 22:329–333.
40. Deschenes MR, Kraemer WJ. Performance and physiologic adaptations to resistance training. *Am J Phys Med Rehabil.* 2002; 81:S3–16. [PubMed: 12409807]
41. Llewellyn ME, Barretto RPJ, Delp SL, Schnitzer MJ. Minimally invasive high-speed imaging of sarcomere contractile dynamics in mice and humans. *Nature.* 2008; 454:784–788. [PubMed: 18600262]
42. Cromie MJ, Sanchez GN, Schnitzer MJ, Delp SL. Sarcomere lengths in human extensor carpi radialis brevis measured by microendoscopy. *Muscle & Nerve.* 2013; 48:286–292. [PubMed: 23813625]
43. Asakawa DS, Pappas GP, Drace JE, Delp SL. Aponeurosis length and fascicle insertion angles of the biceps brachii. *J Mech Med Bio.* 2:449–455.
44. Lieber, RL. *Skeletal Muscle Structure, Function, and Plasticity: The Physiological Basis of Rehabilitation.* M - Medicine Series. Philadelphia: Wolters Kluwer Health/Lippincott Williams & Wilkins; 2009.
45. Huxley HE, Hanson J. Changes in the cross-striations of muscle during contraction and stretch and their structural interpretation. *Nature.* 1954; 173:973–976. [PubMed: 13165698]
46. Kho AL, Perera S, Alexandrovich A, Gautel M. The sarcomeric cytoskeleton as a target for pharmacological intervention. *Curr Opin Pharmacol.* 2012; 12:347–354. [PubMed: 22483604]
47. Caiozzo V. Plasticity of skeletal muscle phenotype: mechanical consequences. *Muscle Nerve.* 2002; 26:740–768. [PubMed: 12451599]
48. Hill AV. The heat of shortening and dynamics constants of muscles. *Proc R Soc Lond B.* 1938; 126:136–195.
49. Millard M, Uchida T, Seth A, Delp SL. Flexing computational muscle: modeling and simulation of musculotendon dynamics. *J Biomech Eng.* 2013; 135:021005. [PubMed: 23445050]
50. Thelen DG. Adjustment of muscle mechanics model parameters to simulate dynamic contractions in older adults. *J Biomech Eng.* 2003; 125:70–77. [PubMed: 12661198]
51. Tskhovrebova L, Trinick J, Sleep JA, Simmons R. Elasticity and unfolding of single molecules of the giant muscle protein titin. *Nature.* 1997; 387:308–312. [PubMed: 9153398]
52. Gautel M. Cytoskeletal protein kinases: titin and its relations in mechanosensing. *Pflugers Arch.* 2011; 462:119–134. [PubMed: 21416260]
53. Magid A, Law D. Myofibrils bear most of the resting tension in frog skeletal muscle. *Science.* 1985; 230:1280–1282. [PubMed: 4071053]
54. Gajdosik RL. Passive extensibility of skeletal muscle: review of the literature with clinical implications. *Clin Biomech.* 2001; 16:87–101.

55. Patel T, Lieber R. Force transmission in skeletal muscle: from actomyosin to external tendons. *Exerc Sport Sci Rev.* 1996; 25:321–363. [PubMed: 9213097]
56. Bustamante AC, Marko JF, Siggia ED, Smith S. Entropic Elasticity of Lambda-Phage DNA. *Science.* 1994; 265:1599–1600. [PubMed: 8079175]
57. Prado LG, Makarenko I, Andresen C, Krüger M, Opitz Ca, et al. Isoform diversity of giant proteins in relation to passive and active contractile properties of rabbit skeletal muscles. *J Gen Physiol.* 2005; 126:461–80. [PubMed: 16230467]
58. Granzier, H.; Helmes, M.; Cazorla, O.; McNabb, M.; Labeit, D., et al. *Elastic Filaments Cell.* Vol. 481. Springer; 2000. Mechanical properties of titin isoforms; p. 283-304.
59. Wang K, Ramirez-Mitchell R. A network of transverse and longitudinal intermediate filaments is associated with sarcomeres of adult vertebrate skeletal muscle. *J Cell Biol.* 1983; 96:562–570. [PubMed: 6682107]
60. Shah SB, Su FC, Jordan K, Milner DJ, Fridén J, et al. Evidence for increased myofibrillar mobility in desmin-null mouse skeletal muscle. *J Exp Biol.* 2002; 205:321–325. [PubMed: 11854369]
61. Peters D, Barash IA, Burdi M, Yuan PS, Mathew L, et al. Asynchronous functional, cellular and transcriptional changes after a bout of eccentric exercise in the rat. *J Physiol.* 2003; 553:947–957. [PubMed: 14514871]
62. Bottinelli R, Canepari M, Pellegrino M, Reggiani C. Force-velocity properties of human skeletal muscle fibres: myosin heavy chain isoform and temperature dependence. *J Physiol.* 1996; 495:573–586. [PubMed: 8887767]
63. Sherwood L. *Human physiology: from cells to systems.* 2010
64. Gordon A, Huxley A, Julian F. The variation in isometric tension with sarcomere length in vertebrate muscle fibres. *J Physiol.* 1966; 184:170–192. [PubMed: 5921536]
65. Blemker SS, Pinsky PM, Delp SL. A 3D model of muscle reveals the causes of nonuniform strains in the biceps brachii. *J Biomech.* 2005; 38:657–665. [PubMed: 15713285]
66. Pette D, Staron RS. Myosin isoforms, muscle fiber types, and transitions. *Microsc Res Tech.* 2000; 50:500–509. [PubMed: 10998639]
67. Scott W, Stevens J, BinderMacleod S. Human skeletal muscle fiber type classifications. *Phys Ther.* 2001; 81:1810–1816. [PubMed: 11694174]
68. Goldspink G, Yang SY. Gene expression associated with muscle adaptation in response to physical signals. *Cell Mol Response to Stress.* 2001; 2:87–96.
69. Thomason D, Booth F. Atrophy of the soleus muscle by hindlimb unweighting. *J Appl Physiol.* 1990; 68:1–12. [PubMed: 2179205]
70. Gregory P, Low RB, Stirewalt WS. Changes in skeletal-muscle myosin isoenzymes with hypertrophy and exercise. *Biochem J.* 1986; 238:55–63. [PubMed: 2948496]
71. Tesch P. Skeletal muscle adaptations consequent to long-term heavy resistance exercise. *Med Sci Sports Exerc.* 1988; 20:S132–S134. [PubMed: 3057312]
72. Huijing PA. Muscle as a collagen fiber reinforced composite: a review of force transmission in muscle and whole limb. *J Biomech.* 1999; 32:329–345. [PubMed: 10213024]
73. Purslow PP, Trotter JA. The morphology and mechanical properties of endomysium in series-fibred muscles: variations with muscle length. *J Muscle Res Cell Motil.* 1994; 15:299–308. [PubMed: 7929795]
74. Smith LR, Lee KS, Ward SR, Chambers HG, Lieber RL. Hamstring contractures in children with spastic cerebral palsy result from a stiffer extracellular matrix and increased in vivo sarcomere length. *J Physiol.* 2011; 589:2625–2639. [PubMed: 21486759]
75. Holzapfel GA. *Nonlinear solid mechanics: a continuum approach for engineering.* 2000
76. Holzapfel GA, Gasser TC, Ogden RW. A new constitutive framework for arterial wall mechanics and a comparative study of material models. *Journal of Elasticity.* 2000; 61:1–48.
77. Purslow PP. Strain-induced reorientation of an intramuscular connective tissue network: implications for passive muscle elasticity. *J Biomech.* 1989; 22:21–31. [PubMed: 2914969]
78. Yucesoy CA, Koopman BHFJM, Baan GC, Grootenboer HJ, Huijing PA. Effects of inter- and extra-muscular myofascial force transmission on adjacent synergistic muscles: assessment by experiments and finite-element modeling. *J Biomech.* 2003; 36:1797–1811. [PubMed: 14614933]

79. Storm C, Pastore JJ, MacKintosh FC, Lubensky TC, Janmey PA. Nonlinear elasticity in biological gels. *Nature*. 2005; 435:191–194. [PubMed: 15889088]
80. Münster S, Jawerth LM, Leslie Ba, Weitz JI, Fabry B, et al. Strain history dependence of the nonlinear stress response of fibrin and collagen networks. *Proc Natl Acad Sci*. 2013; 110:12197–202. [PubMed: 23754380]
81. Wickiewicz T, Roy R. Muscle architecture of the human lower limb. *Clin Orthop Relat Res*. 1983; 179:275–283. [PubMed: 6617027]
82. Schenk P, Siebert T, Hiepe P, Güllmar D, Reichenbach JR, Wick C, Blickhan R, Bäl M. Determination of three-dimensional muscle architectures: validation of the DTI-based fiber tractography method by manual digitization. *J Anatomy*. 223:61–68.
83. De Deyne P. Lengthening of muscle during distraction osteogenesis. *Clin Orthop Relat Res*. 2002; 403S:S171–S177. [PubMed: 12394466]
84. Elsalanty M, Makarov M, Cherkashin A, Birch J, Samchukov M. Changes in pennate muscle architecture after gradual tibial lengthening in goats. *Anat Rec (Hoboken)*. 2007; 290:461–467. [PubMed: 17373691]
85. Makarov M, Birch J, Samchukov M. The role of variable muscle adaptation to limb lengthening in the development of joint contractures: an experimental study in the goat. *J Pediatr Orthop*. 2009; 29:175–181. [PubMed: 19352244]
86. Simpson A, Williams P. The response of muscle to leg lengthening. *J Bone Jt Surg*. 1995; 77:630–636.
87. Pontén E, Fridén J. Immobilization of the rabbit tibialis anterior muscle in a lengthened position causes addition of sarcomeres in series and extra-cellular matrix proliferation. *J Biomech*. 2008; 41:1801–1804. [PubMed: 18460410]
88. Williams PE, Goldspink G. Longitudinal growth of striated muscle fibres. *J Cell Sci*. 1971; 9:751–767. [PubMed: 5148015]
89. Pattullo MC, Cotter MA, Cameron NE, Barry JA. Effects of lengthened immobilization on functional and histochemical properties of rabbit tibialis anterior muscle. *Exp Physiol*. 1992; 77:433–442. [PubMed: 1632953]
90. Nordez A, Casari P, Mariot JP, Cornu C. Modeling of the passive mechanical properties of the musculoarticular complex: acute effects of cyclic and static stretching. *J Biomech*. 2009; 42:767–773. [PubMed: 19264311]
91. Gajdosik RL, Allred JD, Gabbert HL, Sonsteng BA. A stretching program increases the dynamic passive length and passive resistive properties of the calf muscle-tendon unit of unconditioned younger women. *Eur J Appl Physiol*. 2007; 99:449–454. [PubMed: 17186300]
92. Nordez A, Cornu C, McNair P. Acute effects of static stretching on passive stiffness of the hamstring muscles calculated using different mathematical models. *Clin Biomech*. 2006; 21:755–760.
93. LaRoche DP, Connolly DAJ. Effects of stretching on passive muscle tension and response to eccentric exercise. *Am J Sports Med*. 2006; 34:1000–1007. [PubMed: 16476913]
94. Nakamura M, Ikezoe T, Takeno Y, Ichihashi N. Effects of a 4-week static stretch training program on passive stiffness of human gastrocnemius muscle-tendon unit in vivo. *Eur J Appl Physiol*. 2012; 112:2749–2755. [PubMed: 22124523]
95. Reid DA, McNair PJ. Passive Force, Angle, and Stiffness Changes after Stretching of Hamstring Muscles. *Med Sci Sport Exerc*. 2004; 36:1944–1948.
96. Goldspink G. Changes in muscle mass and phenotype and the expression of autocrine and systemic growth factors by muscle in response to stretch and overload. *J Anat*. 1999; 194:323–334. [PubMed: 10386770]
97. Williams PE, Goldspink G. Changes in sarcomere length and physiological properties in immobilized muscle. *J Anat*. 1978; 127:459–468. [PubMed: 744744]
98. Williams PE, Goldspink G. The effect of immobilization on the longitudinal growth of striated muscle fibres. *J Anat*. 1973; 116:45–55. [PubMed: 4798240]
99. Williams P, Catanese T. The importance of stretch and contractile activity in the prevention of connective tissue accumulation in muscle. *J Anat*. 1988; 158:109–114. [PubMed: 3225214]

100. Williams P, Goldspink G. Connective tissue changes in immobilised muscle. *J Anat.* 1984; 138:343–350. [PubMed: 6715254]
101. Gossman MR, Sahrman SA, Rose SJ. Review of length-associated changes in muscle. Experimental evidence and clinical implications. *Phys Ther.* 1982; 62:1799–1808. [PubMed: 6755499]
102. Fry AC. The role of resistance exercise intensity on muscle fibre adaptations. *Sports Med.* 2004; 34:663–679. [PubMed: 15335243]
103. Talmadge R, Roy R. MHC and sarcoplasmic reticulum protein isoforms in functionally overloaded cat plantaris muscle fibers. *J Appl Physiol.* 1996; 80:1296–1303. [PubMed: 8926259]
104. Hubbard R, Ianuzzo C, Linduska J. Compensatory adaptation of skeletal muscle composition to a long term functional overload. *Growth.* 1975; 39:85–93. [PubMed: 1132777]
105. Moore DR, Phillips SM, Babraj JA, Smith K, Rennie MJ. Myofibrillar and collagen protein synthesis in human skeletal muscle in young men after maximal shortening and lengthening contractions. *Am J Physiol Endocrinol Metab.* 2005; 288:E1153–E1159. [PubMed: 15572656]
106. Mackey A, Holm L, Reitelseder S, Pedersen TG, Doessing S, et al. Myogenic response of human skeletal muscle to 12 weeks of resistance training at light loading intensity. *Scand J Med Sci Sports.* 2011; 21:773–782. [PubMed: 21143306]
107. Kirby TJ, McCarthy JJ. MicroRNAs in skeletal muscle biology and exercise adaptation. *Free Radic Biol Med.* 2013; 64:95–105. [PubMed: 23872025]
108. Erskine RM, Jones DA, Williams AG, Stewart CE, Degens H. Resistance training increases in vivo quadriceps femoris muscle specific tension in young men. *Acta Physiol.* 2010; 199:83–89.
109. Kubo K, Ikebukuro T, Yata H. Time course of changes in muscle and tendon properties during strength training and detraining. *J Strength Cond Res.* 2010; 24:322–331. [PubMed: 19996769]
110. Pansarasa O, Rinaldi C, Parente V, Miotti D, Capodaglio P, et al. Resistance training of long duration modulates force and unloaded shortening velocity of single muscle fibres of young women. *J Electromyogr Kinesiol.* 2009; 19:e290–e300. [PubMed: 18801662]
111. Kraemer WJ, Nindl BC, Ratamess NA, Gotshalk LA, Volek JS, et al. Changes in Muscle Hypertrophy in Women with Periodized Resistance Training. *Med Sci Sport Exerc.* 2004; 36:697–708.
112. Shoenle TC, Stelzer JE, Garner DP, Widrick JJ. Functional adaptability of muscle fibers to long-term resistance exercise. *Med Sci Sports Exerc.* 2003; 35:944–951. [PubMed: 12783042]
113. Andersen J, Aagaard P. Myosin heavy chain IIX overshoot in human skeletal muscle. *Muscle Nerve.* 2000; 23:1095–1104. [PubMed: 10883005]
114. Janecki D, Jarocka E, Jaskólska A. Muscle passive stiffness increases less after the second bout of eccentric exercise compared to the first bout. *J Sci Med Sport.* 2011; 14:338–343. [PubMed: 21414841]
115. Seger JY, Arvidsson B, Thorstensson A. Specific effects of eccentric and concentric training on muscle strength and morphology in humans. *Eur J Appl Physiol Occup Physiol.* 1998; 79:49–57. [PubMed: 10052660]
116. Yu JG, Carlsson L, Thornell LE. Evidence for myofibril remodeling as opposed to myofibril damage in human muscles with DOMS: an ultrastructural and immunoelectron microscopic study. *Histochem Cell Biol.* 2004; 121:219–227. [PubMed: 14991331]
117. Simoneau JA, Lortie G, Boulay MR, Marcotte M, Thibault MC, et al. Human skeletal muscle fiber type alteration with high-intensity intermittent training. *Eur J Appl Physiol Occup Physiol.* 1985; 54:250–253. [PubMed: 4065109]
118. Miller BF, Olesen JL, Hansen M, Døssing S, Crameri RM, et al. Coordinated collagen and muscle protein synthesis in human patella tendon and quadriceps muscle after exercise. *J Physiol.* 2005; 567:1021–1033. [PubMed: 16002437]
119. Ianuzzo C, Gollnick P, Armstrong R. Compensatory adaptations of skeletal muscle fiber types to a long-term functional overload. *Life Sci.* 1976; 19:1517–1524. [PubMed: 994700]
120. McDonagh MJN, Davies CTM. Adaptive response of mammalian skeletal muscle to exercise with high loads. *Eur J Appl Physiol.* 1984; 52:139–155.
121. Seynnes OR, Maganaris CN, de Boer MD, di Prampero PE, Narici MV. Early structural adaptations to unloading in the human calf muscles. *Acta Physiol.* 2008; 193:265–274.

122. de Boer MD, Maganaris CN, Seynnes OR, Rennie MJ, Narici MV. Time course of muscular, neural and tendinous adaptations to 23 day unilateral lower-limb suspension in young men. *J Physiol.* 2007; 583:1079–1091. [PubMed: 17656438]
123. Hanson AM, Harrison BC, Young MH, Stodieck LS, Ferguson VL. Longitudinal characterization of functional, morphologic, and biochemical adaptations in mouse skeletal muscle with hindlimb suspension. *Muscle Nerve.* 2012; 48:393–402. [PubMed: 23893872]
124. Ogneva IV. Transversal stiffness of fibers and desmin content in leg muscles of rats under gravitational unloading of various durations. *J Appl Physiol.* 2010; 109:1702–1709. [PubMed: 20829498]
125. Deschenes M. A comparison of the effects of unloading in young adult and aged skeletal muscle. *Med Sci Sports Exerc.* 2001; 33:1477–1483. [PubMed: 11528335]
126. Allen D, Linderman J. Growth hormone/IGF-I and/or resistive exercise maintains myonuclear number in hindlimb unweighted muscles. *J Appl Physiol.* 1997; 83:1857–1861. [PubMed: 9390955]
127. Canon F, Goubel F. Changes in stiffness induced by hindlimb suspension in rat soleus muscle. *Pflugers Arch.* 1995; 429:332–337. [PubMed: 7761257]
128. Widrick JJ, Trappe SW, Romatowski JG, Riley Da, Costill DL, et al. Unilateral lower limb suspension does not mimic bed rest or spaceflight effects on human muscle fiber function. *J Appl Physiol.* 2002; 93:354–360. [PubMed: 12070225]
129. Kasper CE, Xun L. Expression of Titin in Skeletal Muscle Varies with Hind-Limb Unloading. *Biol Res Nurs.* 2000; 2:107–115. [PubMed: 11337816]
130. Toursel T, Stevens L, Granzier H, Mounier Y. Passive tension of rat skeletal soleus muscle fibers: effects of unloading conditions. *J Appl Physiol.* 2002; 92:1465–1472. [PubMed: 11896011]
131. Goto K, Okuyama R, Honda M, Uchida H, Akema T, et al. Profiles of connectin (titin) in atrophied soleus muscle induced by unloading of rats. *J Appl Physiol.* 2003; 94:897–902. [PubMed: 12391127]
132. Berg HE, Eiken O, Miklavcic L, Mekjavic IB. Hip, thigh and calf muscle atrophy and bone loss after 5-week bedrest inactivity. *Eur J Appl Physiol.* 2007; 99:283–289. [PubMed: 17186305]
133. Akima H, Kubo K, Imai M, Kanehisa H, Suzuki Y, et al. Inactivity and muscle: effect of resistance training during bed rest on muscle size in the lower limb. *Acta Physiol Scand.* 2001; 172:269–278. [PubMed: 11531648]
134. Bamman M, Clarke M. Impact of resistance exercise during bed rest on skeletal muscle sarcopenia and myosin isoform distribution. *J Appl Physiol.* 1998; 84:157–163. [PubMed: 9451630]
135. Berg H, Larsson L, Tesch P. Lower limb skeletal muscle function after 6 wk of bed rest. *J Appl Physiol.* 1997; 82:182–188. [PubMed: 9029214]
136. Widrick J, Romatowski J, Bain J, Trappe S, Trappe T, et al. Effect of 17 days of bed rest on peak isometric force and unloaded shortening velocity of human soleus fibers. *Am J Physiol Physiol.* 1997; 273:C1690–C1699.
137. Trappe S, Trappe T, Gallagher P, Harber M, Alkner B, et al. Human single muscle fibre function with 84 day bed-rest and resistance exercise. *J Physiol.* 2004; 557:501–513. [PubMed: 15064323]
138. Ye F, Baligand C, Keener JE, Vohra R, Lim W, et al. Hindlimb muscle morphology and function in a new atrophy model combining spinal cord injury and cast immobilization. *J Neurotrauma.* 2013; 30:227–235. [PubMed: 22985272]
139. Oliveira Milani J, Matheus J, Gomide L, Volpon J, Shimano A. Biomechanical effects of immobilization and rehabilitation on the skeletal muscle of trained and sedentary rats. *Ann Biomed Eng.* 2008; 36:1641–1648. [PubMed: 18683054]
140. D’Antona G, Pellegrino MA, Adami R, Rossi R, Carlizzi CN, et al. The effect of ageing and immobilization on structure and function of human skeletal muscle fibres. *J Physiol.* 2003; 552:499–511. [PubMed: 14561832]
141. Gibson JNA, Halliday D, Morrison WL, Stoward PJ, Hornsby GA, et al. Decrease in human quadriceps muscle protein turnover consequent upon leg immobilization. *Clin Sci.* 1987; 72:503–509. [PubMed: 2435445]

142. Fitts RH, Trappe SW, Costill DL, Gallagher PM, Creer A, et al. Prolonged space flight-induced alterations in the structure and function of human skeletal muscle fibres. *J Physiol.* 2010; 588:3567–3592. [PubMed: 20660569]
143. Widrick JJ, Knuth ST, Norenberg KM, Romatowski JG, Bain JL, et al. Effect of a 17 day spaceflight on contractile properties of human soleus muscle fibres. *J Physiol.* 1999; 516:915–930. [PubMed: 10200437]
144. Caiozzo V, Haddad F, Baker M, Herrick R, Prietto N, et al. Microgravity-induced transformations of myosin isoforms and contractile properties of skeletal muscle. *J Appl Physiol.* 1996; 81:123–132. [PubMed: 8828654]
145. Edgerton V, Zhou M, Ohira Y, Klitgaard H, Jiang B, et al. Human fiber size and enzymatic properties after 5 and 11 days of spaceflight. *J Appl Physiol.* 1995; 78:1733–1739. [PubMed: 7649906]
146. Zhou M, Klitgaard H, Saltin B, Roy R, Edgerton V, et al. Myosin heavy chain isoforms of human muscle after short-term spaceflight. *J Appl Physiol.* 1995; 78:1740–1744. [PubMed: 7649907]
147. Caiozzo V, Baker M, Baldwin K. Modulation of myosin isoform expression by mechanical loading: role of stimulation frequency. *J Appl Physiol.* 1997; 82:211–218. [PubMed: 9029218]
148. Kraus W, Torgan C, Taylor D. Skeletal muscle adaptation to chronic low-frequency motor nerve stimulation. *Exerc Sport Sci Rev.* 1994; 22:313–360. [PubMed: 7925548]
149. Grossman EJ, Roy RR, Talmadge RJ, Zhong H, Edgerton VR. Effects of inactivity on myosin heavy chain composition and size of rat soleus fibers. *Muscle Nerve.* 1998; 21:375–389. [PubMed: 9486867]
150. Roy RR, Baldwin KM, Edgerton VR. The Plasticity of Skeletal Muscle: Effects of Neuromuscular Activity. *Exerc Sport Sci Rev.* 1991; 19:269–312. [PubMed: 1936088]
151. Fournier M, Roy R, Perham H, Simard C, Edgerton V. Is limb immobilization a model of muscle disuse? *Exp Neurol.* 1983; 80:147–156. [PubMed: 6832266]
152. Ausoni S, Gorza L, Schiaffino S, Gundersen K, Lomo T. Expression of myosin heavy chain isoforms in stimulated fast and slow rat muscles. *J Neurosci.* 1990; 10:153–160. [PubMed: 2405110]
153. Neagoe C, Opitz CA, Makarenko I, Linke WA. Gigantic variety: expression patterns of titin isoforms in striated muscles and consequences for myofibrillar passive stiffness. *J Muscle Res Cell Motil.* 2003; 24:175–189. [PubMed: 14609029]
154. Caiozzo VJ, Utkan A, Chou R, Khalafi A, Chandra H, et al. Effects of Distraction on Muscle Length: Mechanisms Involved in Sarcomerogenesis. *Clin Orthop Relat Res.* 2002; 403:S133–S145. [PubMed: 12394462]
155. Lieber R, Friden J. Functional and clinical significance of skeletal muscle architecture. *Muscle Nerve.* 2000; 23:1647–1666. [PubMed: 11054744]
156. Burkholder TJ, Lieber RL. Sarcomere number adaptation after retinaculum transection in adult mice. *J Exp Biol.* 1998; 201:309–316.
157. Goldspink D. The influence of passive stretch on the growth and protein turnover of the denervated extensor digitorum longus muscle. *Biochem J.* 1978; 174:595–602. [PubMed: 708412]
158. Burkholder TJ, Fingado B, Baron S, Lieber RL. Relationship between muscle fiber types and sizes and muscle architectural properties in the mouse hindlimb. *J Morphol.* 1994; 221:177–90. [PubMed: 7932768]
159. Potier TG, Alexander CM, Seynnes OR. Effects of eccentric strength training on biceps femoris muscle architecture and knee joint range of movement. *Eur J Appl Physiol.* 2009; 105:939–944. [PubMed: 19271232]
160. MacDougall J, Sale D, Elder G, Sutton J. Physiology of Elite Powerlifters and Bodybuilders. *Eur J Appl Physiol Occup Physiol.* 1982; 48:117–126. [PubMed: 7199447]
161. Lee SJ, McPherron AC. Regulation of muscle activity and muscle growth. *Proc Natl Acad Sci.* 2001; 98:9306–9311. [PubMed: 11459935]
162. Yokogawa M, Yamazaki T, Inoue K, Inaoka P, Tsuji K, et al. Age-Associated Changes in Atrophy of the Extensor Digitorum Longus Muscle in Hindlimb-Suspended Rats. *J Phys Ther Sci.* 2008; 20:129–133.

163. Allen DL, Roy RR, Edgerton VR. Myonuclear domains in muscle adaptation and disease. *Muscle Nerve*. 1999; 22:1350–1360. [PubMed: 10487900]
164. Ricoy JR, Encinas AR, Cabello A, Madero S, Arenas J. Histochemical study of the vastus lateralis muscle fibre types of athletes. *J Physiol Biochem*. 1998; 54:41. [PubMed: 9732107]
165. Komi PV, Karlsson J. Physical performance, skeletal muscle enzyme activities, and fibre types in monozygous and dizygous twins of both sexes. *Acta Physiol Scand Suppl*. 1979; 462:1. [PubMed: 286499]
166. Mutungi G, Ranatunga KW. The viscous, viscoelastic and elastic characteristics of resting fast and slow mammalian (rat) muscle fibres. *J Physiol*. 1996; 496:827–836. [PubMed: 8930847]
167. Kovanen V, Suominen H, Peltonen L. Effects of aging and life-long physical training on collagen in slow and fast skeletal muscle in rats. A morphometric and immunohistochemical study. *Cell Tissue Res*. 1987; 248:247–255. [PubMed: 3555832]
168. Ahtikoski A, Koskinen SO, Virtanen P, Kovanen V, Takala TE. Regulation of synthesis of fibrillar collagens in rat skeletal muscle during immobilization in shortened and lengthened positions. *Acta Physiol Scand*. 2001; 172:131–140. [PubMed: 11442453]
169. Akesson W, Amiel D, Mechanic G, Woo S, Harwood F, et al. Cross-linking alterations in joint contractures: changes in the reducible cross-links in periarticular connective tissue collagen after nine weeks of immobilization. *Connect Tissue Res*. 1977; 5:15–19. [PubMed: 141358]
170. Woo S, Matthews J, Akesson W, Amiel D, Convery F. Connective tissue response to immobility. *Arthritis Rheum*. 1975; 18:257–264. [PubMed: 1137613]
171. Kubo K, Kanehisa H. Influence of static stretching on viscoelastic properties of human tendon structures in vivo. *J Appl Physiol*. 2001; 90:520–527. [PubMed: 11160050]
172. Magnusson SP, Narici MV, Maganaris CN, Kjaer M. Human tendon behaviour and adaptation, in vivo. *J Physiol*. 2008; 586:71–81. [PubMed: 17855761]
173. Röhrle O, Davidson JB, Pullan A. A physiologically based, multi-scale model of skeletal muscle structure and function. *Front Physiol*. 2012; 3:1–14. [PubMed: 22275902]
174. Gillies AR, Lieber RL. Structure and function of the skeletal muscle extracellular matrix. *Muscle Nerve*. 2011; 44:318–331. [PubMed: 21949456]
175. Booth FW, Thomason DB. Molecular and cellular adaptation of muscle in response to exercise: perspectives of various models. *Physiol Rev*. 1991; 71:541–585. [PubMed: 2006222]
176. Fowles J, MacDougall J, Tarnopolsky M, Sale D, Roy B, et al. The effects of acute passive stretch on muscle protein synthesis in humans. *Can J Appl Physiol*. 2000; 25:165–180. [PubMed: 10932034]
177. Sandler, H. Inactivity: physiological effects. Elsevier; 1986.
178. Kawakami Y. Muscle-fiber pennation angles are greater in hypertrophied than in normal muscles. *J Appl Physiol*. 1993; 74:2740–2744. [PubMed: 8365975]
179. Kawakami Y, Abe T, Kuno SY, Fukunaga T. Training-induced changes in muscle architecture and specific tension. *Eur J Appl Physiol Occup Physiol*. 1995; 72:37–43. [PubMed: 8789568]
180. Maxwell LC, Faulkner JA, Hyatt GJ. Estimation of number of fibers in guinea pig skeletal muscles. *J Appl Physiol*. 1974; 37:259–264. [PubMed: 4851910]
181. Blemker SS, Delp SL. Three-Dimensional Representation of Complex Muscle Architectures and Geometries. *Ann Biomed Eng*. 2005; 33:661–673. [PubMed: 15981866]
182. Böl M, Reese S. Micromechanical modelling of skeletal muscles based on the finite element method. *Comput Methods Biomech Biomed Eng*. 2008; 11:489–504.
183. Böl M. Micromechanical modelling of skeletal muscles: from the single fiber to the whole muscle. *Arch Appl Mech*. 2010; 80:557–567.
184. Röhrle O, Davidson J, Pullan A. Bridging scales: a three-dimensional electromechanical finite element model of skeletal muscle. *SIAM J Sci Comput*. 2008; 30:2882–2904.
185. Röhrle O. Simulating the electro-mechanical behavior of skeletal muscles. *Comput Sci Eng*. 2010; 12:48–58.
186. Oomens C, Maenhout M, van Oijen C, Drost M, Baaijens F. Finite Element Modelling of Contracting Skeletal Muscle. *Philos Trans R Soc Lond B Biol Sci*. 2003; 358:1453–1460. [PubMed: 14561336]

187. Lemos RR, Epstein M, Herzog W, Wyvill B. A framework for structured modeling of skeletal muscle. *Comput Methods Biomech Biomed Engin.* 2004; 7:305–317. [PubMed: 15621651]
188. Dash RK, Dibella Ja, Cabrera ME. A computational model of skeletal muscle metabolism linking cellular adaptations induced by altered loading states to metabolic responses during exercise. *Biomed Eng Online.* 2007; 6:14. [PubMed: 17448235]
189. Murtada SC, Arner A, Holzapfel GA. Experiments and mechanochemical modeling of smooth muscle contraction: Significance of filament overlap. *J Theor Bio.* 2012; 297:176–186. [PubMed: 22108241]
190. Taber LA. Biomechanical growth laws for muscle tissue. *J Theor Bio.* 1998; 193:201–213. [PubMed: 9714932]
191. Kuhl E. Growing matter - A review of growth in living systems. *J Mech Behavior Biomed Mat.* 29:529–543.
192. Wren T. A computational model for the adaptation of muscle and tendon length to average muscle length and minimum tendon strain. *J Biomech.* 2003; 36:1117–1124. [PubMed: 12831737]
193. Zöllner AM, Abilez O, Böl M, Kuhl E. Stretching skeletal muscle: Chronic muscle lengthening through sarcomerogenesis. *PLoS One.* 2012; 7:e45661. [PubMed: 23049683]
194. Göktepe S, Abilez OJ, Kuhl E. A generic approach towards finite growth with examples of athlete's heart, cardiac dilation, and cardiac wall thickening. *J Mech Phys Solids.* 2010; 58:1661–1680.
195. Böl M, Leichsenring K, Weichert C, Sturmat M, Schenk P, Blickhan R, Siebert T. Three-dimensional surface geometries of the rabbit soleus muscle during contraction: input for biomechanical modeling and its validation. *Biomech Model Mechanobio.* 12:1205–1220.
196. Ambrosi D, Ateshian GA, Arruda EM, Cowin SC, Dumais J, Goriely A, Holzapfel GA, Humphrey JD, Kemkemer R, Kuhl E, Olberding JE, Taber LA, Garikipati K. Perspectives on biological growth and remodeling. *J Mech Phys Solids.* 59:863–883. [PubMed: 21532929]
197. Göktepe S, Abilez OJ, Parker KK, Kuhl E. A multi-scale model for eccentric and concentric cardiac growth through sarcomerogenesis. *J Theor Bio.* 265:433–442. [PubMed: 20447409]
198. Matano T, Tamai K, Kurokawa T. Adaptation of skeletal muscle in limb lengthening: a light diffraction study on the sarcomere length in situ. *J Orthop Res.* 1994; 12:193–196. [PubMed: 8164091]
199. Arnold EM, Delp SL. Fibre operating lengths of human lower limb muscles during walking. *Phil Trans R Soc B.* 2011; 366:1530–1539. [PubMed: 21502124]
200. Rausch MK, Dam A, Gktepe S, Abilez OJ, Kuhl E. Computational modeling of growth: Systemic and pulmonary hypertension in the heart. *Biomech Mod Mechanobio.* 2011; 10:799–811.
201. DeFreitas JM, Beck TW, Stock MS, Dillon MA, Kasishke PR. An examination of the time course of training-induced skeletal muscle hypertrophy. *Eur J Appl Physiol.* 2011; 111:2785–2790. [PubMed: 21409401]
202. Gruther W, Benesch T, Zorn C, Paternostro-Sluga T, Quittan M, et al. Muscle wasting in intensive care patients: ultrasound observation of the M. quadriceps femoris muscle layer. *J Rehabil Med.* 2008; 40:185–189. [PubMed: 18292919]
203. Kuhl E, Holzapfel GA. A continuum model for remodeling in living structures. *J Mat Sci.* 2007; 42:8811–8823.
204. Saez P, Pena E, Martinez MA, Kuhl E. Mathematical modeling of collagen turnover in biological tissue. *J Math Bio.* 2013; 67:1765–1793. [PubMed: 23129392]
205. Delp SL, Zajac FE. Force- and moment-generating capacity of lower-extremity muscles before and after tendon lengthening. *Clin Ortho Rel Res.* 1992; 284:247–259.
206. Blemker SS, Delp SL. Rectus femurs and vast us intermedius fiber excursions predicted by three-dimensional muscle models. *J Biomech.* 2006; 39:1383–1391. [PubMed: 15972213]
207. Joo ST, Kim GD, Hwang YH, Ryu YC. Control of fresh meat quality through manipulation of muscle fiber characteristics. *Meat Science.* 2013; 95:828–836. [PubMed: 23702339]
208. Reeves ND, Maganaris CN, Longo S, Narici MV. Differential adaptations to eccentric versus conventional resistance training in older humans. *Exp Physiol.* 2009; 94:825–833. [PubMed: 19395657]

209. Eriksson A, Kadi F, Malm C, Thornell LE. Skeletal muscle morphology in power-lifters with and without anabolic steroids. *Histochem Cell Biol.* 2005; 124:167–175. [PubMed: 16059740]

Author Manuscript

Author Manuscript

Author Manuscript

Author Manuscript

molecular **subcellular** **cellular** **tissue** **organ**
[nm] [um] [mm] [cm] [dm]

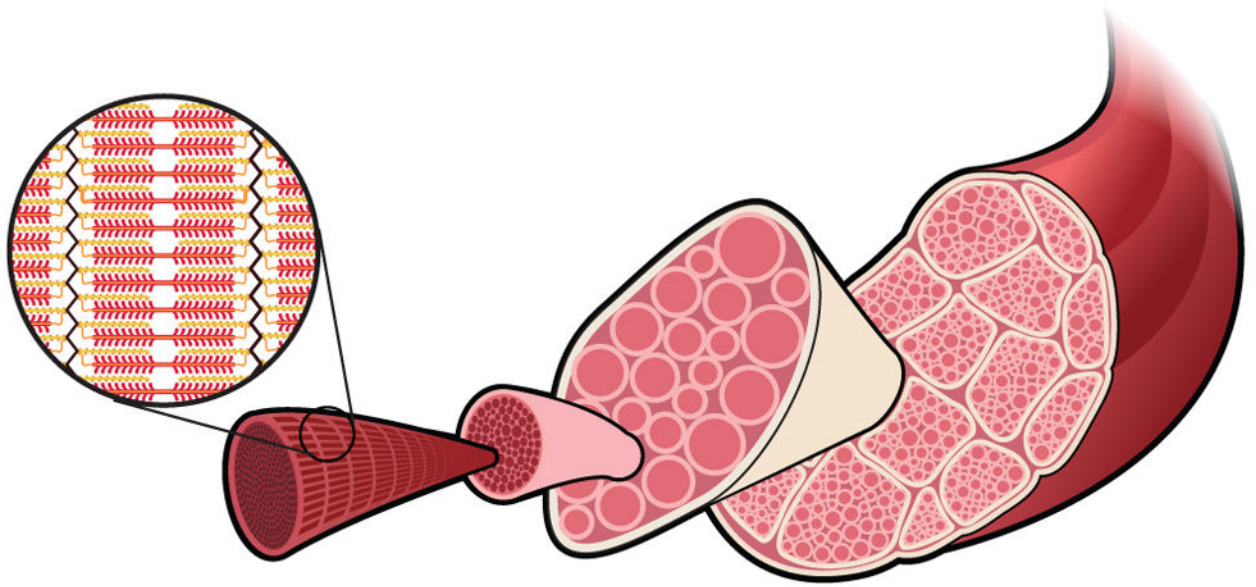


Fig. 1. Length scales of skeletal muscle adaptation. Muscle adaptation to mechanical stimuli spans from the molecular to the organ scale, bridging eight orders of magnitude in length.

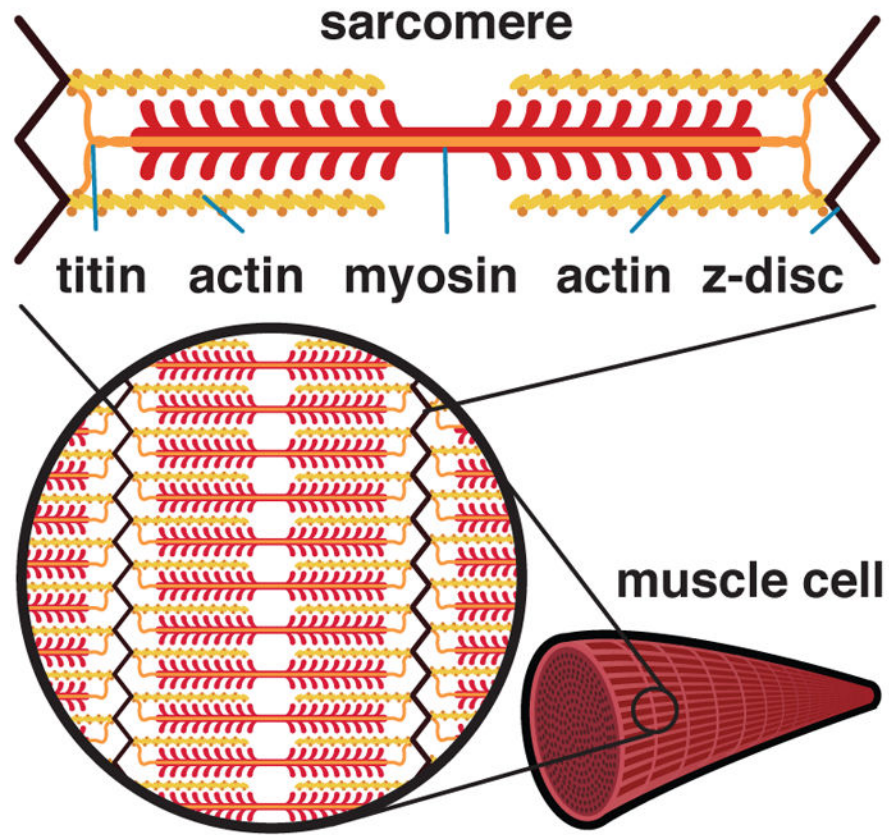


Fig. 2.

Anatomy and physiology on the molecular and sub-cellular scales. The sarcomere is defined as the region between two Z-discs. The Z-disc is connected to myosin via titin. To generate force, myosin filament heads ratchet along actin filaments. The myosin heavy chain isoform influences the intrinsic velocity of active force generation. The titin filament primarily affects the passive fiber force.

active fiber force vs. velocity for varying fiber types

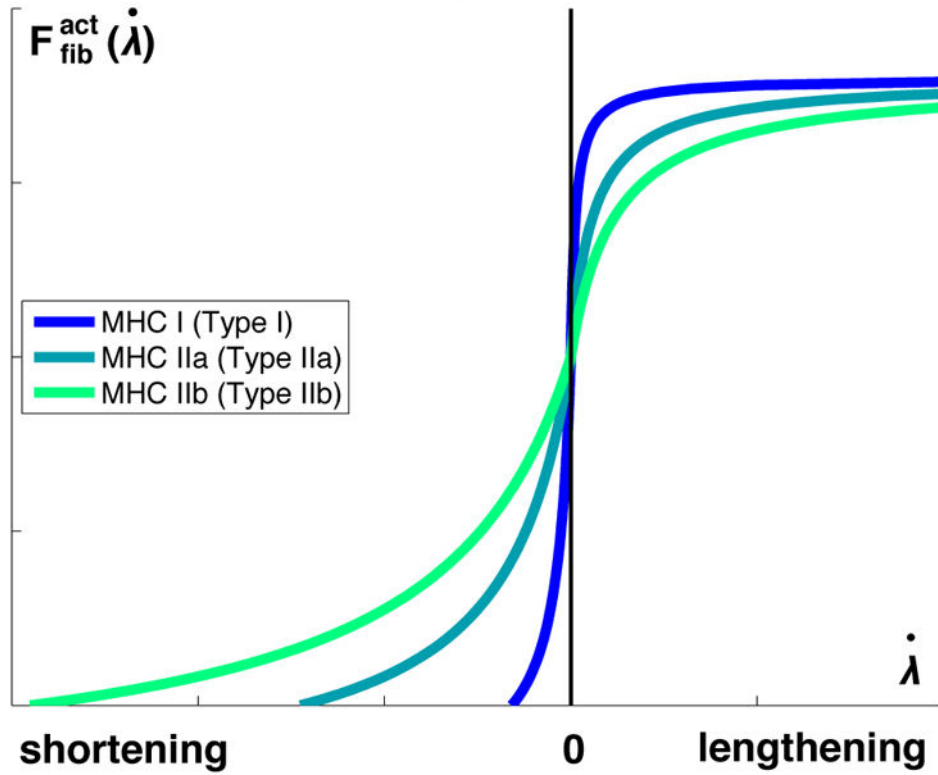


Fig. 3.

Active fiber force $F_{\text{fib}}^{\text{act}}$ vs. velocity $\dot{\lambda}$ for different myosin heavy chain isoforms. Myosin heavy chain Type I is associated with slow isoforms; myosin heavy chain Types IIa and IIb are associated with fast isoforms.

passive fiber force vs. stretch for varying titin isoforms

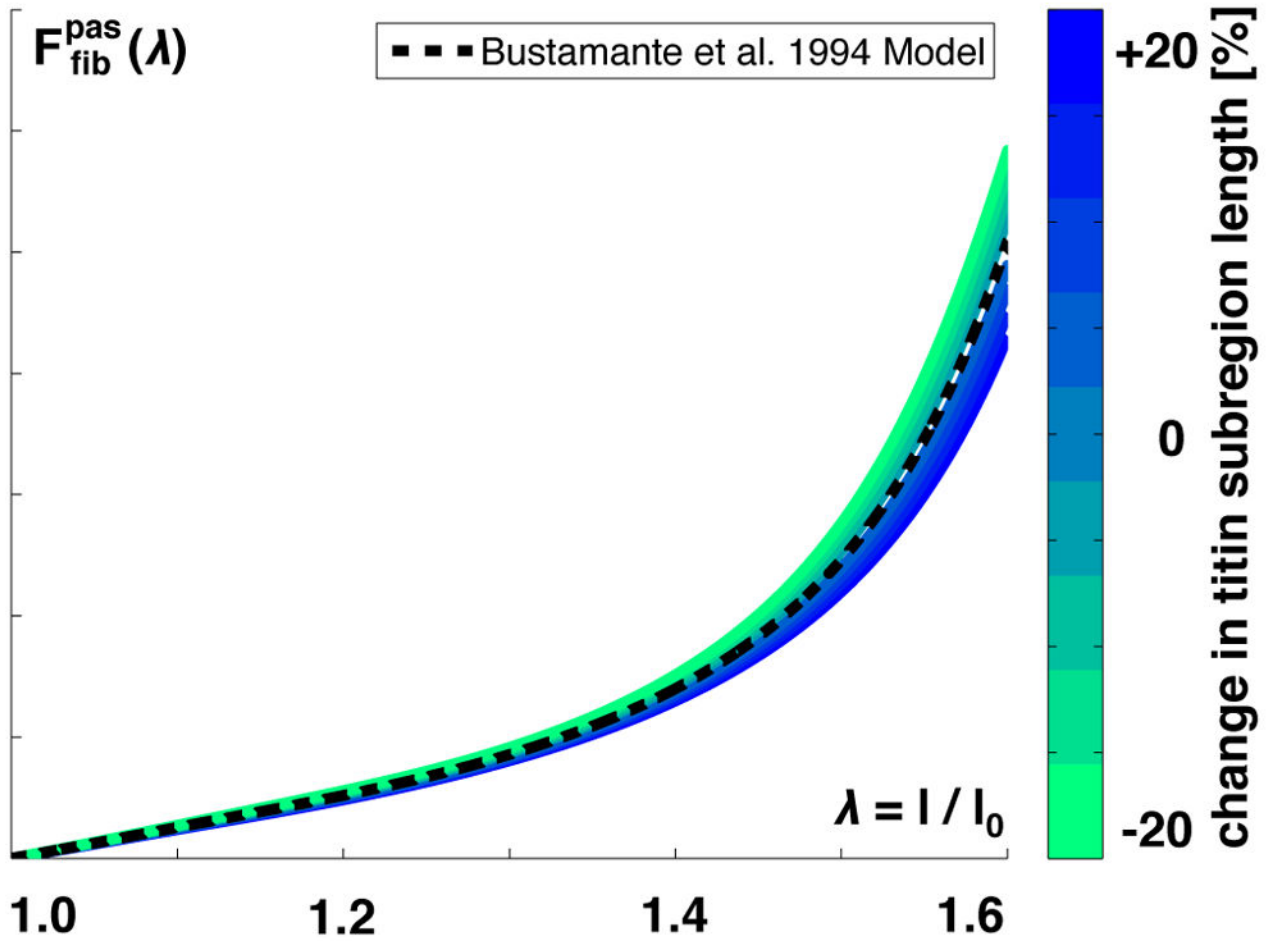


Fig. 4.

Passive fiber force F_{fib}^{pas} vs. fiber stretch λ . The passive force increases exponentially with increasing stretch, reflecting the wormlike chain behavior of titin. Increasing or decreasing the stretch of a titin subregion, shown in blue and green, increases or decreases the passive force in the fiber direction.

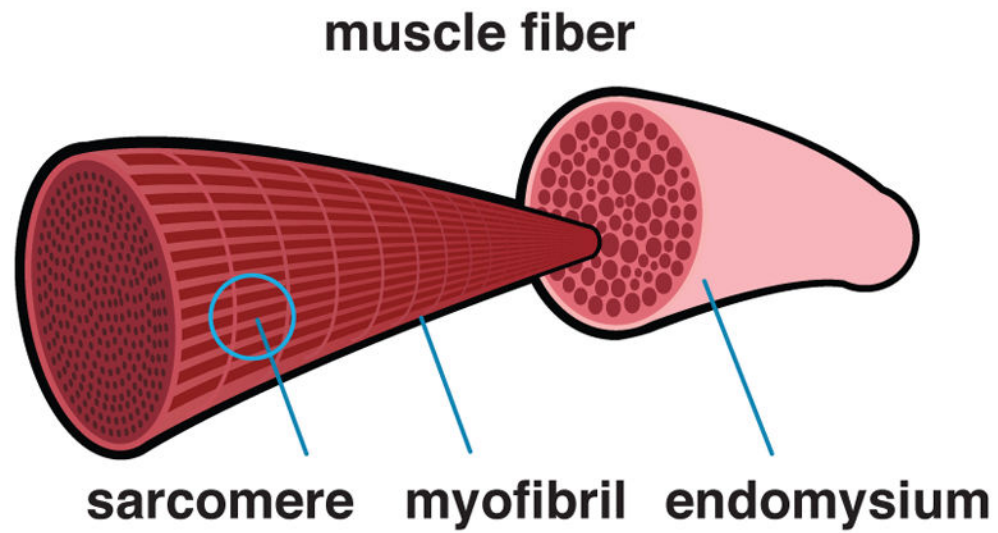


Fig. 5. Anatomy and physiology on the cellular scale. Sarcomeres arranged in series form myofibrils, which, arranged in parallel, make up the muscle cell or muscle fiber. Muscle fibers are surrounded by endomysium.

active fiber force vs. stretch for varying fiber length

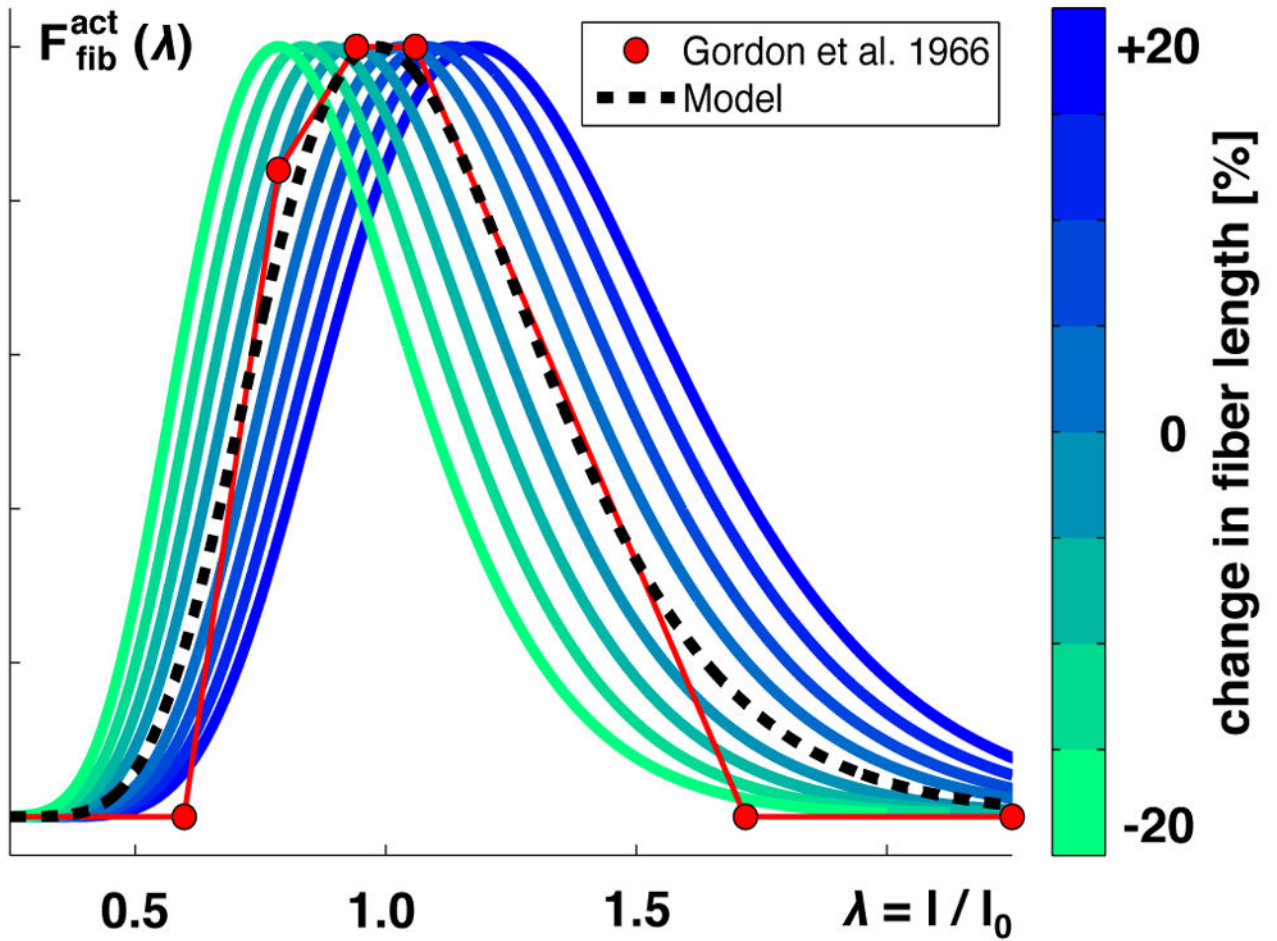


Fig. 6.

Active fiber force $F_{\text{fib}}^{\text{act}}$ vs. fiber stretch λ . The active force increases toward the optimal fiber length and then decays. Adding or removing sarcomeres in series, shown in blue and green, increases or decreases the optimal fiber length. Modeled force predicts experimentally measured force shown in red [64].

active fiber force vs. stretch for varying cross sectional area

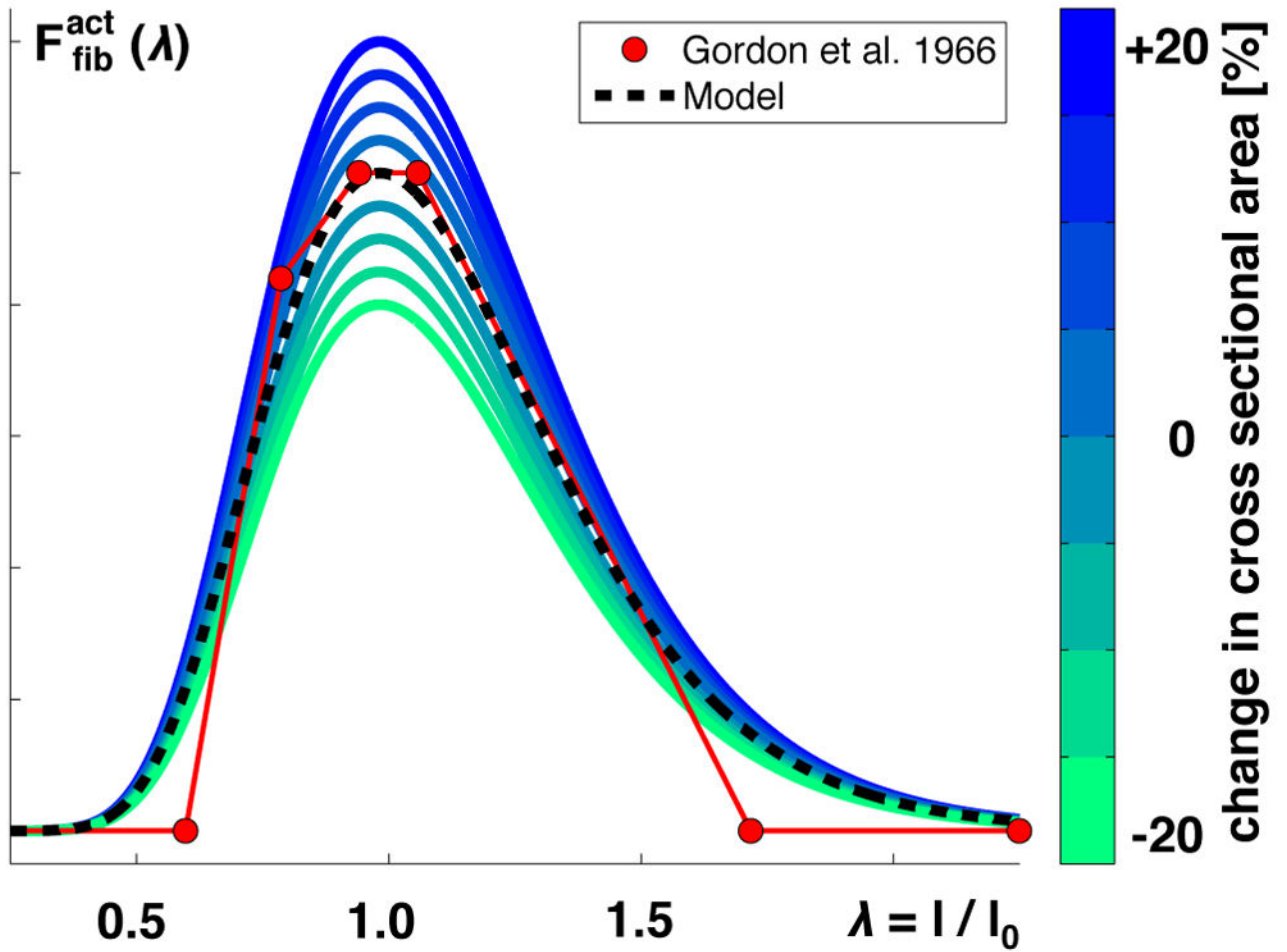


Fig. 7.

Active fiber force $F_{\text{fib}}^{\text{act}}$ vs. fiber stretch λ . The active force increases toward the optimal fiber length and then decays. Adding or removing sarcomeres in parallel, shown in blue and green, increases or decreases the fiber cross sectional area, which increases or decreases the active fiber force. Modeled force predicts experimentally measured force shown in red [64].

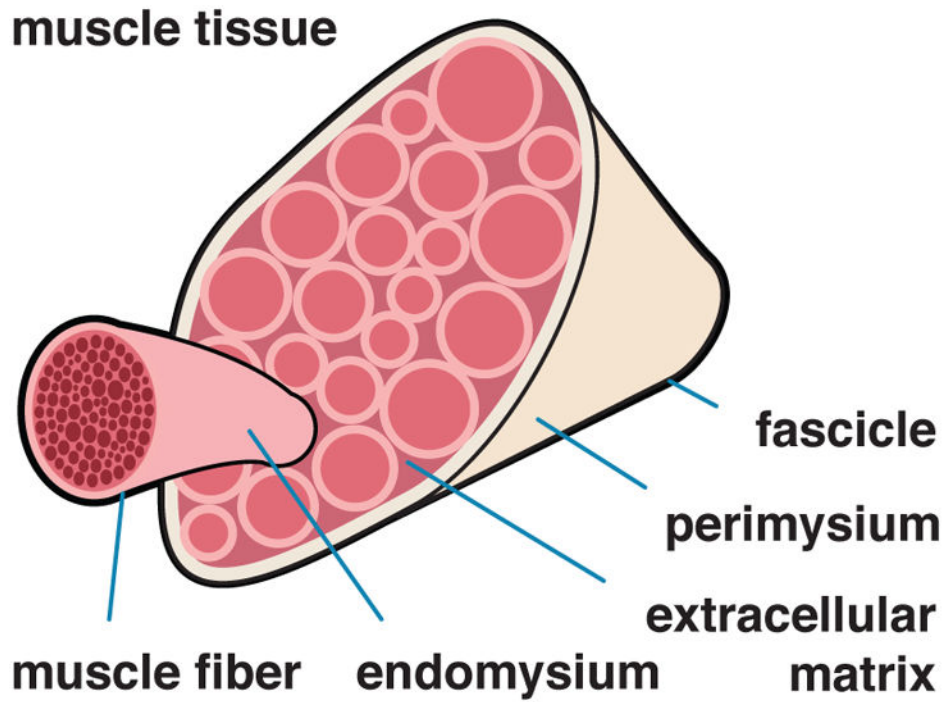


Fig. 8. Anatomy and physiology on the tissue scale. Muscle fibers, embedded in a collagenous extracellular matrix, form a fascicle. Muscle fibers are surrounded by the endomysium, fascicles are surrounded by the perimysium, and the whole muscle is surrounded by epimysium.

passive matrix force vs. stretch for varying matrix stiffness

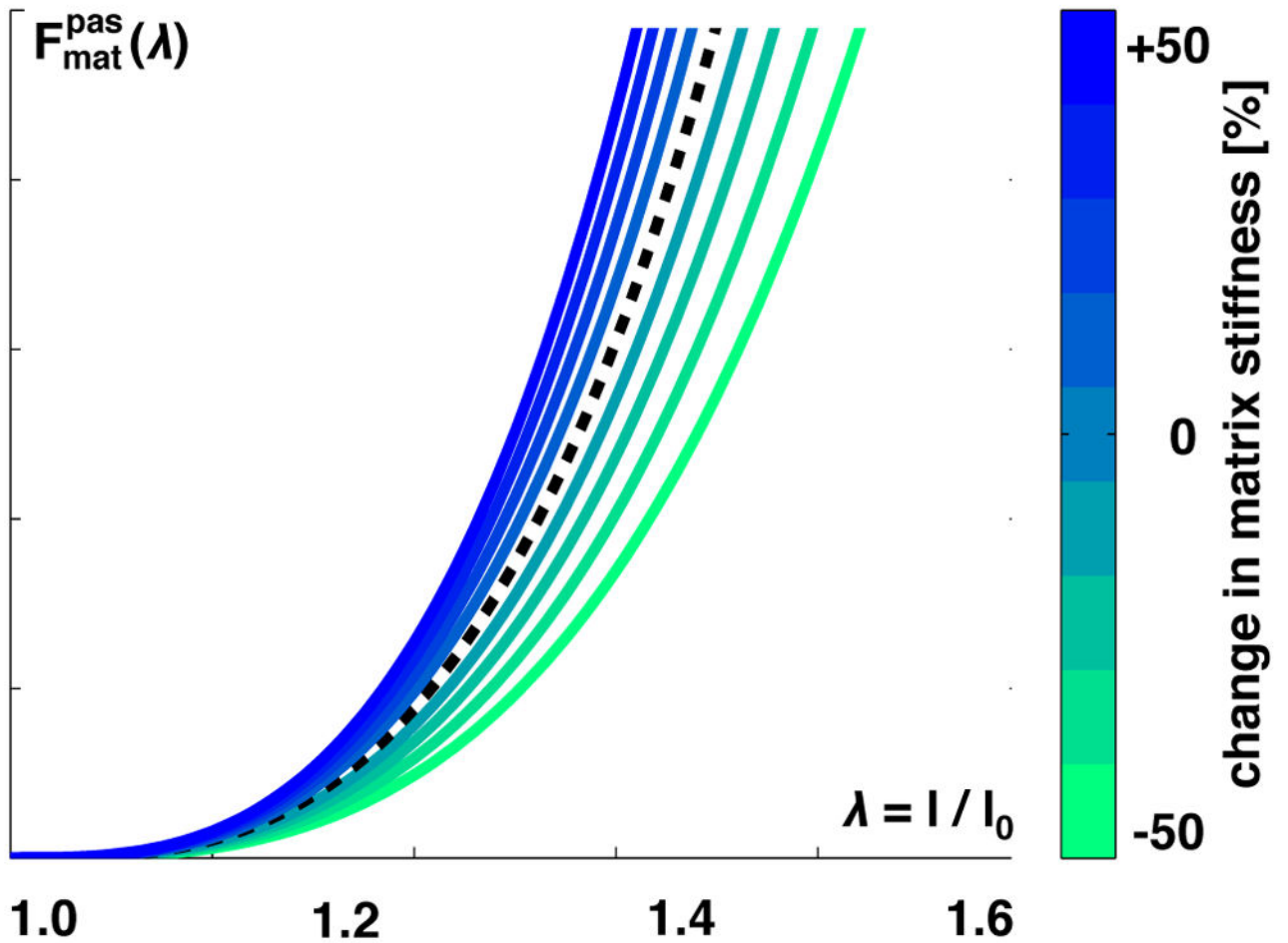


Fig. 9.

Passive extracellular matrix force $F_{\text{mat}}^{\text{pas}}$ vs. extracellular matrix tissue stretch λ . The passive force increases exponentially with increasing stretch, reflecting collagen fiber untangling and stiffening. Increasing or decreasing the collagen content increases or decreases the matrix stiffness, shown in blue and green, and increases or decreases the passive force.

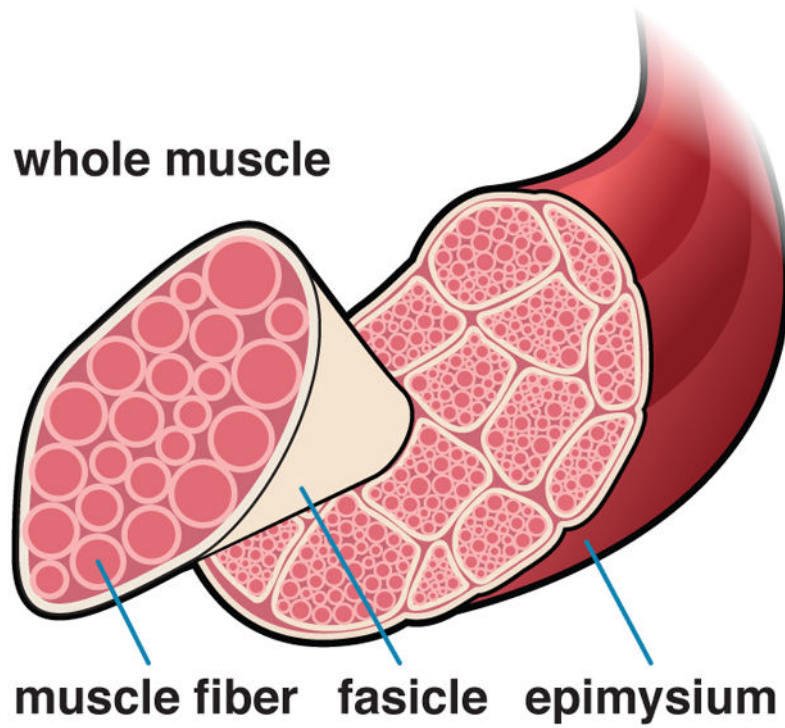


Fig. 10. Anatomy and physiology on the organ scale. A bundle of fascicles are contained within the epimysium, the outermost connective tissue layer, to form the whole muscle.

total muscle force vs. stretch

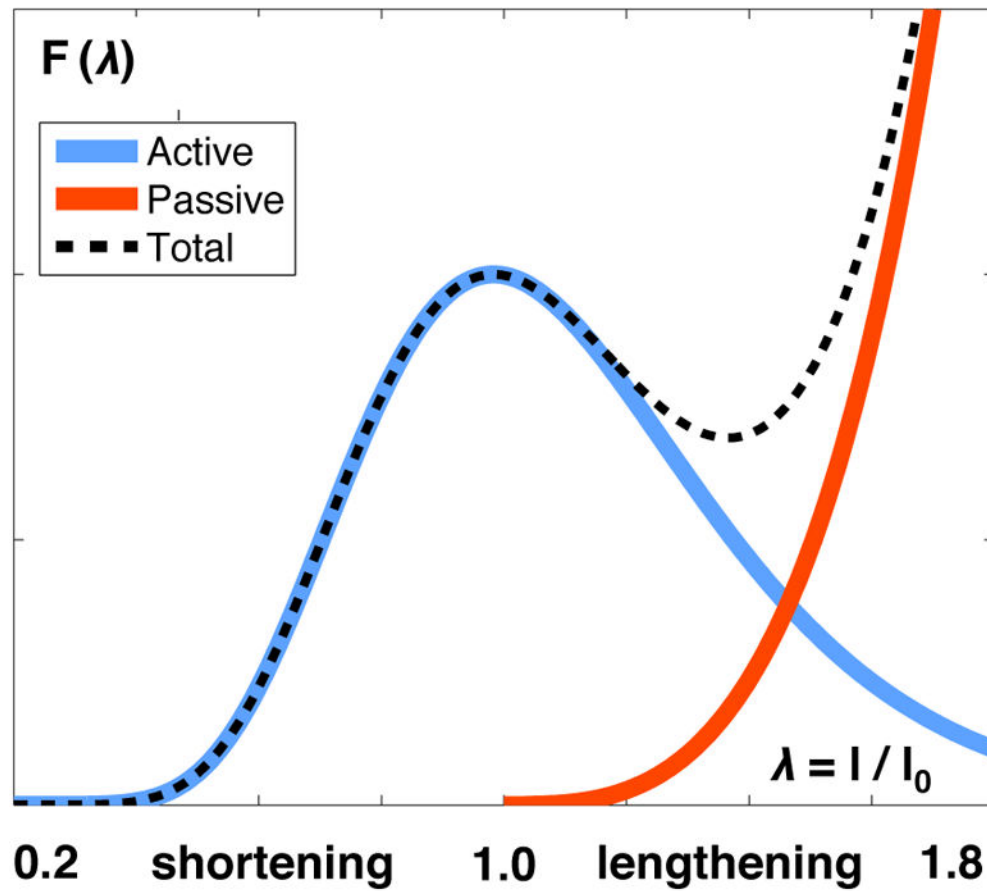


Fig. 11. Total muscle force F vs. muscle stretch λ . As the sum of the active and passive forces F_{act} and F_{pas} , the total muscle force peaks and drops in agreement with the active force and then stiffens drastically in agreement with the passive force.

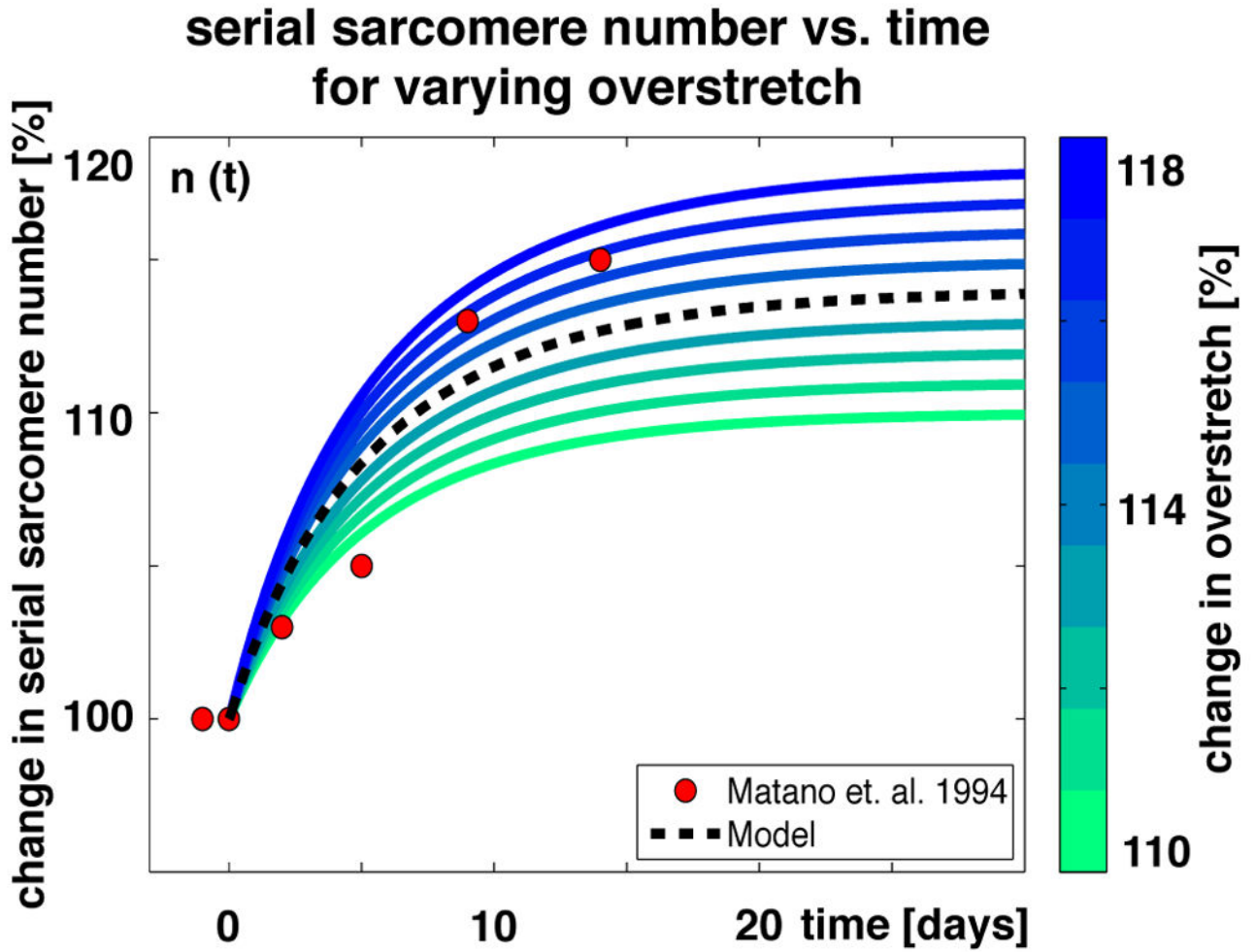


Fig. 12.

Serial sarcomere number vs. time. The serial sarcomere number increases exponentially and converges toward a homeostatic equilibrium, which depends on the applied overstretch. Increasing or decreasing the overstretch, shown in blue and green, increases or decreases the serial sarcomere number. Modeled sarcomere numbers, shown as black dashed line, show the same trend as experimentally measured sarcomere numbers, shown as red circles [198].

cross sectional area vs. time for varying overload

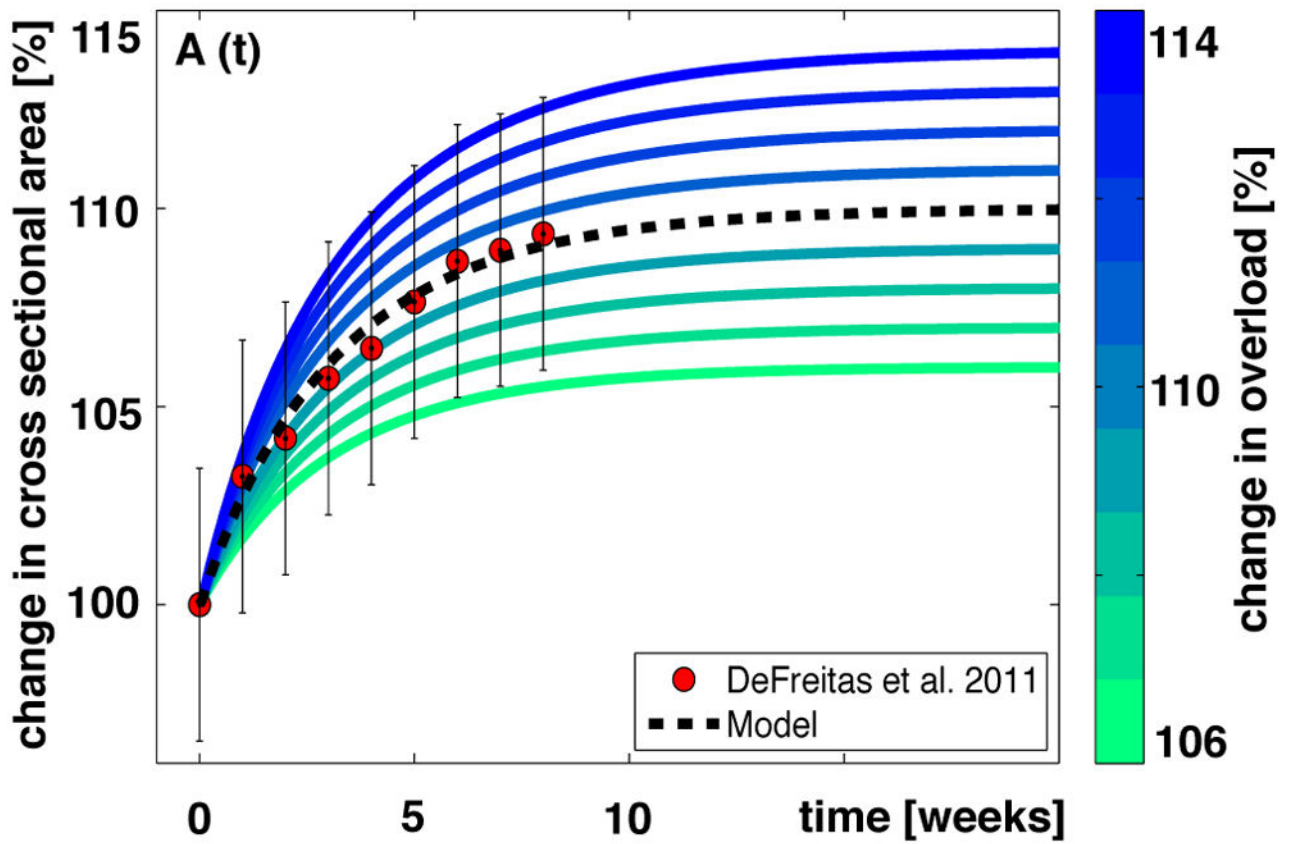


Fig. 13.

Cross sectional area vs. time. The cross sectional area increases exponentially and converges toward a homeostatic equilibrium, which depends on the applied overload. Increasing or decreasing the overload, shown in blue and green, increases or decreases the cross sectional area. Modeled cross sectional areas, shown as black dashed line, predict experimentally measured cross sectional areas, shown as red circles [201].

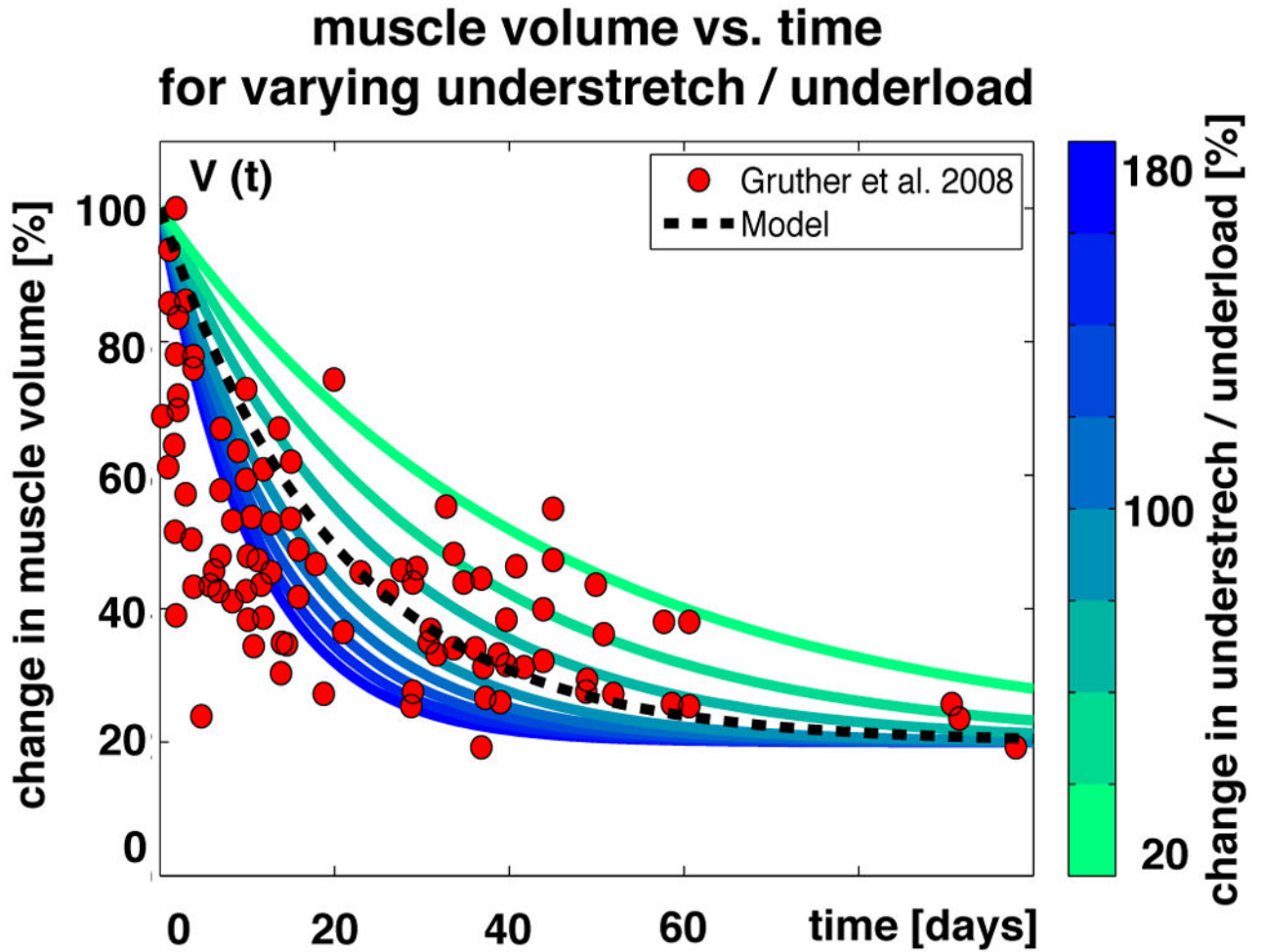






Fig. 14.

Muscle volume vs. time. The muscle volume decreases exponentially and converges toward a homeostatic equilibrium. The speed of muscle loss depends on the degree disuse or underload. Increasing or decreasing the underload, shown in blue and green, increases or decreases the speed of muscle loss. Modeled muscle loss, shown as black dashed line, shows the same trend as experimentally measured muscle loss, shown as red circles [202].

Table 1

Overview of mechanical stimuli, observed adaptations, and key literature.

Stimulus	Mechanism	Molecular & Subcellular	Cellular	Tissue	Organ
Overstretch 	Limb Lengthening [13, 14, 23, 83-86], Immobilization in Lengthened Position [8, 20, 87-89], Stretch Regimen [90-96]	Sarcomeres in series ↑ [13, 14, 20, 83, 85, 86, 88] Sarcomere length ↑ [84, 85] Slower MHC ↑ [8, 10]	Fiber Length ↑ [14, 84, 85] Slower Fiber Type ↑ [10, 89]	Passive Stiffness ↑ [23, 95], Mixed [92], NC [91, 93] ECM ↑ [87] Collagen ↑ [23]	Penmation Angle ↓ [84] Fascicle Length ↑ [13, 23, 84, 86]
Understretch 	Immobilization in shortened position [6, 19-21, 88, 97-100], Postural Misalignment and Muscle Imbalance [101], Tenotomy [21]	Sarcomeres in series ↓ [6, 19-21, 88, 97, 98] Faster MHC ↑ [8]	Fiber CSA ↓ [19]	Passive Stiffness ↑ [20, 24, 97] ECM ↑ [100] Collagen ↑ [100]	Fascicle Length ↓ [6]
Overload 	Functional Overload [11, 102-104], Resistance Exercise [2, 3, 7, 9, 12, 15, 16, 22, 25, 26, 61, 105, 106, 108-118]	Sarcomeres in series: ↑ [15, 16] * [3, 116] (ECC), ↓ [3] (CON) Sarcomeres in parallel ↑ [11, 12, 26, 112] * Slower MHC ↑ [7, 9, 102, 103, 113], NC [26, 110]	Fiber CSA ↑ [11, 12, 26, 112] Fiber f^{max}/CSA ↑ [110] Slower Fiber Type ↑ [113, 117, 119], NC [120]	Passive Stiffness ↑ [22, 25, 114] Collagen ↑ [22, 118]	Anat. CSA ↑ [11, 12, 15, 16, 26, 105, 108, 109, 111, 115] Volume ↑ [26, 108] Penmation Angle ↑ [12, 15, 16, 26, 108] Fascicle Length ↑ [2, 15, 16] Anat. f^{max}/CSA ↑ [108]

Stimulus	Mechanism	Molecular & Subcellular	Cellular	Tissue	Organ
Underload 	Limb Unweighting [4, 5, 113, 121–131], Bed Rest [17, 132–137], Immobilization [4, 18, 138–141], Microgravity [142–145]	Sarcomeres in parallel ↓ [18, 125, 134–136, 141–143]*, [17] Faster MHC ↑ [113, 140, 144, 146], NC [123, 134, 135] Titin length ↓ [129], density ↓ [129, 130], elasticity ↓ [131]	Fiber CSA ↓ [18, 125, 134–136, 141–143], Slow Only [123, 126] Fiber f^{max}/CSA ↓ [110, 128, 136, 137, 140, 143] Faster Fiber Type ↑ [127, 140, 144, 145], NC [18, 134, 135]	Passive Stiffness NC [139]	Anat. CSA ↓ [4, 5, 18, 121, 122, 132, 133] Volume ↓ [4, 5, 121] Pennation Angle ↓ [4, 5, 121, 122] Fascicle Length ↓ [5, 121, 122] Anat. f^{max}/CSA ↓ [18, 121]

Anat. = Anatomical; CON = Concentric; CSA = Cross Sectional Area; ECC = Eccentric; ECM = Extracellular Matrix; MHC = Myosin Heavy Chain; MI = Mixed Results; NC = No Change;

*. inferred from change in fiber dimensions.